

# Key features of Turing systems are determined purely by network topology

Xavier Diego<sup>1,2</sup>, Luciano Marcon<sup>3</sup>, Patrick Müller<sup>3</sup>, and James Sharpe<sup>1,2,4</sup>

<sup>1</sup>EMBL-CRG Systems Biology Research Unit, Center for Genomic Regulation, Barcelona Institute for Science and Technology, Barcelona, Spain

<sup>2</sup>Universitat Pompeu Fabra, Barcelona, Spain

<sup>3</sup>Friedrich Miescher Laboratory of the Max Planck Society, Germany

<sup>4</sup>Institucio Catalana de Recerca i Estudis Avancats, Barcelona, Spain

## Abstract

Turing’s theory of pattern formation is a universal model for self-organization, applicable to many systems in physics, chemistry and biology. Essential properties of a Turing system, such as the conditions for the existence of patterns and the mechanisms of pattern selection are well understood in small networks. However, a general set of rules governing how network topology determines fundamental system properties and constraints has not been found. Here we provide a first general theory of Turing network topology, which proves why three key features of a Turing system are directly determined by the topology: the type of restrictions that apply to the diffusion rates, the robustness of the system, and the phase relations of the molecular species.

## 1 Introduction

The hallmark of biological development is the formation of spatially organized cellular structures. In 1952, Alan Turing proposed a mechanism based on the reaction and diffusion of morphogen molecules that would allow cells to self-organize and form periodic patterns [1]. However, nearly 40 years passed until Turing patterns were observed in the CIMA chemical reaction [2, 3]. The main reason why Turing patterns had been so elusive was that they can not occur if all the molecules diffuse at the same rates [4], as typically occurs in laboratory reactions. Further, Turing models with moderate diffusion ratios require a level of adjustment in the reaction parameters that is unrealistic [5], an issue that has been referred to as the fine-tuning problem [6]. The severity of these requirements has cast doubts about the relevance of Turing patterns in biological systems. In the CIMA reaction, the diffusion constraint was serendipitously circumvented by the introduction of an immobile color indicator that reversibly bound to one of the reactants and slowed down its diffusion [7, 8]. Hindering the diffusion of the activator with a non-diffusible complexing agent was the basis of a method proposed to systematically design new Turing reactions [9]. A refinement of this method [10] has been followed in the design of almost all new chemical systems producing Turing patterns [11] and inspired most of the

theoretical efforts to relax the diffusion constraints in Turing networks [12, 13]. Turing patterns with equal diffusion rates of the diffusible molecules have also been noticed in models of biological pattern formation that include immobile cell membrane receptors as part of the network [14, 15, 16, 17]. These networks have the common feature of relying on the introduction of a non-diffusible node that interacts with the activator but is inert to the other reactants, following the architecture of the original CIMA model.

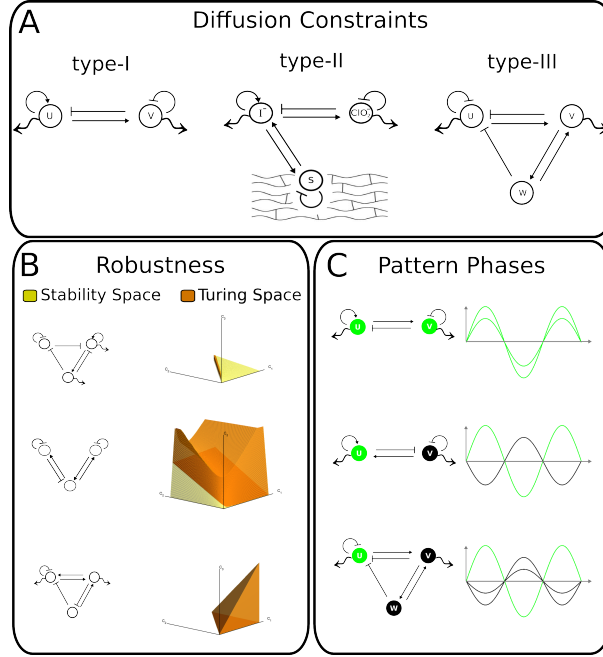


Figure 1: Three questions under investigation a) Why the diffusion rates of  $u$  and  $v$  in the standard 2-node Turing network (left) must be very different, whereas in the CIMA network (center) iodine and chlorite can diffuse at the same rate and in the third (right) network the diffusion rates of  $u$  and  $v$  are completely unconstrained? b) Why the robustness of these three Turing networks is so different? c) What determines the phase of each species in a Turing pattern?

However, in a recent study [18] we have found that the hindered diffusion architecture is just one particular case amongst many other possibilities for the relaxation of diffusion constraints in Turing networks with immobile nodes. Our computational analysis of all possible reaction-diffusion networks of 3 and 4 nodes revealed that they can be classified into three types according to the restrictions that apply to the diffusion rates. The first type comprises networks in which a subset of the species must diffuse at a higher rate than the rest, as is the case in the classical 2-node Turing networks. In the second type, the diffusion rates are subjected to certain constraints but can form Turing patterns even if the diffusion rates of the mobile species are all equal, as in the CIMA reaction [7] and related models [13, 14, 15]. The third type is formed by networks in which the diffusion rates of the mobile species are not subjected to any

constraint, a novel class of Turing networks that had not been found before. These computational results suggested that central aspects of Turing networks have to be clarified.

Here we demonstrate that the type of diffusion constraints that apply to Turing network of any number of nodes are determined by its topology. Topology also explains a new class of pseudo-patterning networks that we call Turing filters. The patterns generated by Turing filters do not have a characteristic wave-length; instead these networks amplify preexisting spatial heterogeneities if their characteristic wavelength is smaller than a critical threshold. Also, the graph analysis allows us to distinguish networks that can undergo oscillatory Turing instabilities, and the classification according to diffusion constraints carries over to these patterning systems. Secondly, the analysis shows that Turing networks can be grouped into a few topological families, and that the robustness associated to the size of their Turing space is largely determined by them. Finally, our analysis allows us to resolve a question that, surprisingly, has not been addressed before: what determines the phase overlaps of the species in a Turing pattern? Again, the graph structure of a network allows us to predict the phases of the species and it shows also how to construct a network with any desired combination of phase overlaps.

## Methods: Graph theory for Turing networks

A network of interacting species whose concentration changes through local reactions and spatial diffusion can be described by a set of reaction-diffusion equations.

$$\frac{\partial r_i}{\partial t} = f_i(r) + d_i \nabla^2 r_i \quad i = 1, \dots, N \quad (1)$$

where  $r_i(x, t)$ ,  $f_i$  and  $d_i \geq 0$  represent the concentrations, reaction rates and non-negative diffusion constants. The system is assumed to be stable without diffusion and there is no flow of reactants outside a finite domain. Generally, diffusion smooths out spatial heterogeneities in these type of systems. Turing's genius intuition [1] consisted in realizing that diffusion could have the opposite effect if the reactants interacted in the appropriate way, so that a spatially periodic pattern would replace the homogeneous state as the stable equilibrium. Existence of Turing patterns is demonstrated by analyzing the evolution of a system under small perturbations, which can be predicted from the linear approximation of the reaction-diffusion equations [19]. This leads to an eigenvalue problem that reduces the derivation of the conditions for diffusion-driven instability to the analysis of the zeroes of the characteristic polynomial  $P_q(\lambda) = \det[\lambda \mathbf{I} - (\mathbf{J}^{\mathbf{R}}(r_o) - q^2 \mathbf{D})]$ , where  $\mathbf{J}^{\mathbf{R}}(r_o)$  is the Jacobian of the reaction term evaluated at equilibrium and  $\mathbf{D}$  is the diffusion matrix. The departure from equilibrium is a superposition of periodic modes of wavenumber  $q$  and speed of growth or decay given by the eigenvalues  $\lambda(q)$ . If the real part of the largest  $\lambda(q)$  is positive, this mode grows exponentially and contributes to the emergence of a Turing pattern. The mode  $q_c$  associated to the eigenvalue with the maximum real part grows faster and dominates the final pattern. If  $\lambda(q_c)$  is real, a stationary pattern with wavelength  $2\pi/q_c$  emerges. If  $\lambda(q_c)$  is complex, an oscillatory pattern emerges with wavelength  $2\pi/q_c$  and oscillation period given by  $2\pi/\text{Im}(\lambda(q_c))$ . The eigenvalues are given by the zeroes of  $P_q(\lambda)$ . For

a network with  $N$  species  $P_q(\lambda)$  is a polynomial of degree  $N$  in  $\lambda$ :

$$P_q(\lambda) = \lambda^N + a_1(q)\lambda^{N-1} + \dots + a_{N-1}(q)\lambda + a_N(q) = 0 \quad (2)$$

where the coefficients  $a_i(q)$  are functions of the kinetic constants and the diffusion rates. The location of the zeroes of a polynomial in the complex plane is given by the Routh-Hurwitz theorem, but simpler conditions to locate them can be derived in terms of the coefficients  $a_k(q)$  [20]. Stability without diffusion requires that all the coefficients of  $P_q(\lambda)$  are positive for  $q = 0$ . Hence  $a_K(0) > 0$  for  $K = 1, \dots, N$  is a necessary condition for stability and, conversely,  $a_K(q) < 0$  for some  $K$  is a sufficient condition for diffusion-driven instabilities. In turn, necessary conditions for the existence of stationary Turing patterns can be derived in terms of the sign of  $a_N(q)$ :

$$\exists q > 0, \forall k < N \quad | \quad \begin{matrix} a_k(q) > 0 \\ a_N(q) < 0 \end{matrix} \quad \Leftarrow \quad \text{stationary Turing} \quad (3)$$

For oscillatory patterns, a similar condition can be derived in terms of  $a_{K < N}(q)$ , but it is only sufficient [21, 22]:

$$\exists q > 0, \exists k < N \quad | \quad \begin{matrix} a_k(q) < 0 \\ a_N(q) > 0 \end{matrix} \quad \Rightarrow \quad \text{oscillatory Turing} \quad (4)$$

A comprehensive discussion of the derivation and scope of the conditions for diffusion-driven instabilities is given in SM1. In principle, the parametric constraints for the existence of Turing patterns can be derived analytically from these conditions. In practice, they become intractable for networks with more than 3 diffusible species.

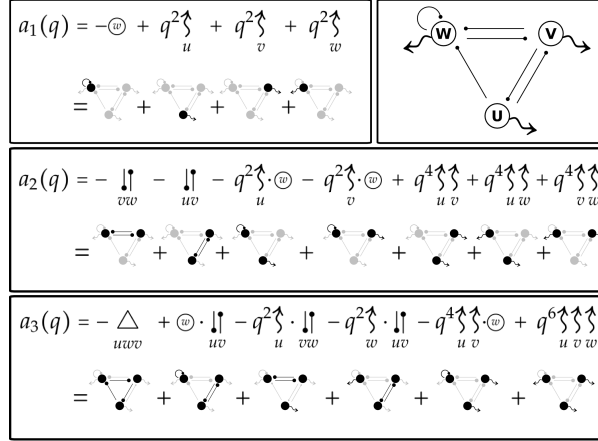


Figure 2: Calculation of  $P_q(\lambda)$  as a sum of  $\ell$ -subgraphs. Nodes, edges and diffusive loops that form each  $\ell$ -subgraph are shown in black. The loop of the  $i$ -th node is represented by  $\odot$  in the equations.

For this reason, we introduce a method based on Graph theory to recast them in terms of the topology of the underlying reaction-diffusion system. In

this way we reveal a connection between the structure of a reaction-diffusion system and diffusion constraints, robustness and pattern phases. To that end, a directed graph is associated to the matrix  $\mathbf{F}^{\text{RD}}(q) = \mathbf{J}^R(r_0) - q^2 \mathbf{D}$  obtained from the linear approximation of the reaction-diffusion equations. Our definition of the reaction-diffusion graph follows the definition of the Coates graph of a square matrix: the graph of a reaction-diffusion network with  $N$  species has  $N$  nodes and an edge from the  $j$ -th node to the  $i$ -th node if the entry  $\mathbf{J}^R(r_0)_{ij}$  is non-zero [23]. The entries on the diagonal of the Jacobian result in edges that start and end in the same node. These edges are called loops and are associated to decay or self-activation terms. In addition, for each non-zero entry in  $\mathbf{D}$ , a special type of loop represented by a wriggled arrow is added to the corresponding diffusible node. The weight of each edge is given by the corresponding entry in  $\mathbf{F}^{\text{RD}}(q)$ . Particularly, the diffusive loop associated to the diffusible node  $i$  has weight  $-q^2 d_i$ . The fundamental elements of the graph are cycles. A cycle of length  $m$  is a set of  $m$  edges that form a closed path joining  $m$  distinct nodes. By this definition, loops are cycles of length one. The weight of a cycle is defined as the product of its edges. Cycles are classified as positive or negative according to the sign of their weight. Two important graph structures are Induced subgraphs and Linear spanning subgraphs, or for short,  $\ell$ -subgraphs. The Induced subgraph of  $k$  nodes is formed by these nodes and all the edges between them. Conversely, the complementary nodes of an induced subgraph of size  $k$  are the  $N - k$  nodes that are not contained in it. An  $\ell$ -subgraph of size  $k$  is a set of disjoint cycles that spans  $k$  nodes and is contained in their Induced subgraph. The weight of an  $\ell$ -subgraph is:

$$w(\ell) = \prod_{c \subseteq \ell} (-w(c)) \quad (5)$$

Thus, the weight of an  $\ell$ -subgraph is positive if it is formed by negative cycles or contains an even number of positive cycles. In this case it is said to be an stabilizing  $\ell$ -subgraph. Examples of cycles, induced and  $\ell$ -subgraphs and the association of the reaction-diffusion graph for a 4-node network are shown in SM2. Importantly,  $\ell$ -subgraphs are the only contributors to  $P_q(\lambda)$ , as it can be proven from the Laplace expansion of the characteristic polynomial [24] and the Coates expression for the determinant [23]. Precisely, the coefficient  $a_k(q)$  is given by the sum of all the  $\ell$ -subgraphs of size  $k$  in the reaction-diffusion graph. The expression of the coefficients of  $P_q(\lambda)$  in terms of subgraphs for a minimal 3-node network is shown 2. The contribution of each Induced subgraph of  $k$  nodes can be separated into a)  $\ell_R$ -subgraphs formed only by reaction cycles b) mixed  $\ell_{RD}$ -subgraphs formed by  $m$  diffusive loops and the complementary  $\ell_R$ -subgraph formed by reaction cycles spanning the other  $k - m$  nodes. c) an  $\ell_D$ -subgraph formed by  $k$  diffusive loops, provided that all the inducing nodes are diffusible:

$$a_k(q) = \sum_{I_{\gamma_k}} \left[ \sum_{\ell_R \subseteq I_{\gamma_k}} w(\ell_R) + \sum_{\gamma_m \subseteq \gamma_k}^{m < k} q^{2m} \left( \prod_{j \in \gamma_m} d_j \right) \cdot \left( \sum_{\ell_R \subseteq I_{\gamma_k - \gamma_m}} w(\ell_R) \right) + q^{2k} \prod_{j \in \gamma_k} d_j \right] \quad (6)$$

Two important results follow from the previous expression. First, the topology of a network, understood as the distribution of cycles, cycle signs and dif-

fusion loops, determines exclusively the requirements for the existence of Turing patterns. The reason is that the conditions for diffusion-driven instability depend on the coefficients  $a_k(q)$  and these are functions of  $\ell$ -subgraphs only. Therefore, the existence of Turing patterns imposes constraints on the relative weights of cycles, rather than individual kinetic parameters. Second, a Turing network must have a destabilizing module: an Induced subgraph in which the destabilizing  $\ell_R$ -subgraphs outweigh the stabilizing  $\ell_R$ -subgraphs. Typically, this condition requires that there is a set of nodes linked by a positive cycle that outweighs any stabilizing  $\ell$ -subgraphs contained in their Induced subgraph. If a network does not have destabilizing module, all the terms in  $a_N(q)$  are positive and the condition 3 for instability can not be fulfilled. A rigorous proof of this result is given in SM3 and constitutes a generalization of the requirement of a self-activator in 2-node Turing networks.

## 2 Results

### 2.1 Topology and the source Diffusion constraints

In our previous work [18] we developed a symbolic algebra procedure to obtain the exhaustive list of 3 and 4-node networks with the minimal number of edges that can generate stationary Turing patterns. The analysis revealed that 3-node and 4-node networks with two diffusible nodes can be classified into three types according to the diffusion constraints for the generation of Turing patterns. Defining the ratio of diffusion rates of the two diffusible species as  $d$ , and  $p$  as the space of kinetic parameters compatible with Turing patterns, the constraints for each Type can be stated as:

$$\begin{aligned} \text{Type - I} &: \forall p \quad d > 1 \\ \text{Type - II} &: \exists p \quad d = 1 \\ \text{Type - III} &: \forall p \quad d > 0 \end{aligned} \tag{7}$$

Surprisingly, we found that there are as many 3-node networks with one immobile reactant of Type-II and Type-III as of Type-I, whereas the 4-node networks with two immobile reactants of Type-III outnumber the networks of Type-I and Type-II. In other words, against the widely held belief, Turing networks with mild or no diffusion constraints are very common. Here we demonstrate how the topology of a network explains these results. According to the stability condition, all the independent terms  $a_k(0)$  in eq.6 are positive. The leading terms in  $a_k(q)$ , if present, are also strictly positive for  $q > 0$ . According to the condition for Turing instability,  $a_N(q)$  must cross the zero and turn negative for some  $q > 0$ . Decartes rule of signs provides an upper bound for the number of real positive zeros of a real polynomial [25]. Particularly, a polynomial with only non-negative coefficients cannot have real positive zeros. It then follows that  $a_N(q)$  must have a negative coefficient, and the negative coefficient must lie at some intermediate degree in  $q^2$ . This is a necessary condition for Turing instabilities. In a network in which all the species diffuse, this is only possible with differential diffusivity. The algebraic proof of this well known result is given in SM9 but it does not reveal the source of the requirement and how it can be weakened. To that end it is necessary to examine how the network graph leads to a nested structure of the characteristic polynomial. As shown in eq.6, the

coefficient of degree  $2m$  in  $a_N(q)$  is the sum of all mixed  $\ell_{RD}$ -subgraphs formed by  $m$  diffusive loops and an  $\ell_R$ -subgraph that spans the other  $N - m$  nodes of the network. Importantly, each of these  $\ell_R$ -subgraphs of size  $N - m$  contribute also to the coefficient  $a_{N-m}(0)$  of  $a_{N-m}(q)$ . For example, in the topology shown in 2 the coefficient  $a_3(q)$  is:

$$a_3(q) = a_3(0) - q^2 \begin{array}{c} \uparrow \\ u \end{array} \cdot \begin{array}{c} \downarrow \\ vw \end{array} - q^2 \begin{array}{c} \uparrow \\ w \end{array} \cdot \begin{array}{c} \downarrow \\ uv \end{array} - q^4 \begin{array}{c} \uparrow \\ u \end{array} \begin{array}{c} \uparrow \\ v \end{array} \begin{array}{c} \downarrow \\ w \end{array} \cdot \begin{array}{c} \circledast \\ uv \end{array} + q^6 \begin{array}{c} \uparrow \\ u \end{array} \begin{array}{c} \uparrow \\ v \end{array} \begin{array}{c} \uparrow \\ w \end{array} \quad (8)$$

Thus, the coefficient of degree  $q^2$  in  $a_3(q)$  contains all the reaction  $\ell_R$ -subgraphs of size 2 that form the independent term  $a_2(0)$  in  $a_2(q)$ . Likewise, the coefficient of degree  $q^4$  in  $a_3(q)$  contains all the loops that form  $a_1(0)$  in  $a_1(q)$ . This illustrates the nested structure of the  $P_q(\lambda)$ :

$$\begin{aligned} a_1(0) &= -\begin{array}{c} \circledast \\ uv \end{array} \\ a_2(0) &= -\begin{array}{c} \uparrow \\ vw \end{array} - \begin{array}{c} \downarrow \\ uv \end{array} \end{aligned} \quad (9)$$

Stability imposes that  $a_k(0) > 0$  and therefore, that the stabilizing subgraphs outweigh the destabilizing subgraphs of size  $k$ . It follows that for any of the coefficients of intermediate degree in  $a_N(q)$  to be negative, the diffusion loops complementary of the destabilizing  $\ell_R$ -subgraphs have to compensate this difference. Thus, the differential diffusion requirement for Turing instabilities stems from the necessary condition derived from Decartes' rule of signs. To illustrate the relationship explicitly, let the Induced subgraph of  $u$  and  $v$  be the destabilizing module in the network from 2, and the cycle of length two between them the only positive cycle. Then, only the coefficient of degree  $q^2$  in  $a_3(q)$  can be negative. Imposing this and assuming for simplicity that the diffusion rates of the nodes in the destabilizing module are equal, the constraint on the diffusion ratio  $d = \zeta_w / \zeta_u = \zeta_w / \zeta_v$  takes the following form:

$$\left. \begin{aligned} -\begin{array}{c} \uparrow \\ vw \end{array} - \begin{array}{c} \downarrow \\ uv \end{array} &> 0 \\ -\begin{array}{c} \uparrow \\ vw \end{array} \cdot \begin{array}{c} \uparrow \\ u \end{array} - \begin{array}{c} \downarrow \\ uv \end{array} \cdot \begin{array}{c} \downarrow \\ w \end{array} &< 0 \end{aligned} \right\} \Rightarrow d > -\begin{array}{c} \uparrow \\ vw \end{array} / \begin{array}{c} \downarrow \\ uv \end{array} > 1 \quad (10)$$

Two observations about the diffusion constraints are in order. First, the constraints on diffusion rates that stem from Decartes' rule are necessary for the existence of Turing patterns, but not sufficient. If the necessary ratio is set, the sufficient conditions are obtained imposing that  $a_N(q)$  turns negative, which results in additional requirements for the kinetic parameters but not for the diffusion rates. Second, the nested structure of the characteristic polynomial and Decartes' rule imposes that at least one of the species complementary to the destabilizing module has a larger diffusion rate than the species that induce it, and never the other way around. This is the generalization of the requirement of differential diffusion between an activator and an inhibitor in 2-node networks: in larger networks, the role of the activator and inhibitor cannot be assigned to individual species, but to network subgraphs. Importantly, the previous argument carries over for general networks of any size but depends on the assumption that all species diffuse. Each coefficient  $a_k(0)$  is formed by all the reaction  $\ell_R$ -subgraphs of size  $k$ . If all species diffuse, each  $\ell_R$ -subgraph in  $a_k(0)$  can be coupled to  $m$  diffusive loops of complementary nodes to form a

mixed  $\ell_{RD}$ -subgraph of size  $k + m$  that contributes to the coefficient of degree  $2m$  in  $a_{k+m}(q)$ . Thus, the nested structure of the characteristic polynomial, from which the diffusion constrains stem, is a general property of networks in which all species diffuse. Because of this, all networks in which all species diffuse belong to the Type-I class.

## Relaxation of diffusion constrains

In networks with immobile species, the nested structure of the characteristic polynomial does not necessarily hold.

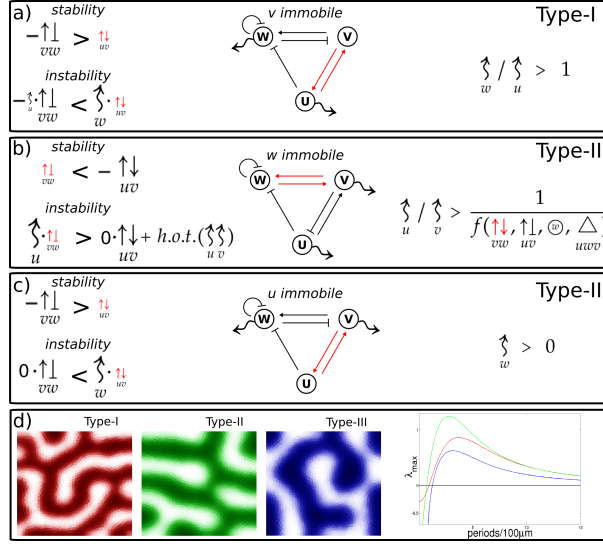


Figure 3: a-c) Permutation of the immobile node in Topology of 2. results in a Turing network of each Type. Stability and instability requirements are shown on the left, diffusion constraints on the right. d) Patterns and dispersion relationships of Type-I, II, III are qualitatively similar (shown in red, green and blue)

This property is lost if there is at least one  $\ell_R$ -subgraph with one or more complementary nodes that are non-diffusible. Assuming that this subgraph is of size  $k$ , it will contribute to  $a_k(0)$  but it will not to  $a_N(q)$ . Particularly, it will be missing from the coefficient of degree  $2m$  in  $a_N(q)$  formed by products of  $\ell_R$ -subgraphs of size  $k$  and  $m = N - k$  diffusion loops of their complementary nodes. If the subgraph that is missing is stabilizing and the destabilizing module is also of size  $k$ , the requirements on the diffusion rates stemming from Decartes rule are weakened. The destabilizing module can outweigh the remaining subgraphs and make the coefficient of degree  $2m$  in  $a_N(q)$  negative, even if the diffusion loops of its complementary nodes are equal or smaller than its own. In this way, the necessary condition of differential diffusivity is weakened. By the same mechanism, subgraphs of smaller size than the destabilizing module might be prevented from contributing to coefficients of higher degree than  $2m$  in  $a_N(q)$ . In turn, this facilitates the fulfillment of the sufficient condition for the



existence of Turing patterns. This is the principle that underlies the relaxation of diffusion constraints and the associated classification of Turing networks. The precise topological characterization of each Turing Type is given in table 1:

Type-I	All stabilizing $\ell_R$ -subgraphs of the same size as the destabilizing module have all their complementary nodes diffusible
Type-II	At least one stabilizing $\ell_R$ -subgraph of the same size as the destabilizing module has an immobile complementary node
Type-III	The destabilizing module is the $\ell_R$ -subgraph of smallest size that has all its complementary nodes diffusible

Table 1: Topological features of Turing networks

The topological properties of the different Turing Types results in algebraic differences that allow to make a simple distinction based on the form of the characteristic polynomial. In Type-III networks the destabilizing module is the only contributor to the leading term in  $a_N(q)$ . Hence, for all modes with wavenumber  $q$  above a certain threshold  $a_N(q)$  turns negative and the system is unstable independently of the diffusion rates. Both the necessary condition derived from Decartes' rule and the sufficient condition  $a_N(q) < 0$  are guaranteed by the topology.

There are two configurations that result in a Type-II network. In the first configuration, the destabilizing module is the only contributor of its size to a coefficient in  $a_N(q)$ , but there are stabilizing subgraphs of smaller size that contribute to the coefficients of larger degree. It follows that the necessary condition is guaranteed by the topology but the sufficient condition still involves the diffusion rates. In the second configuration of Type-II networks, the destabilizing module is not the only contributor to a coefficient in  $a_N(q)$ , but at least one stabilizing subgraph of the same size is missing. Thus, the necessary condition is not guaranteed by the topology, but it can be fulfilled without differential diffusion. Whether there are terms of higher degree or not determines if the sufficient condition is satisfied automatically or if it imposes additional requirements on the kinetic rates. In Type-I networks, all subgraphs of the same size as the destabilizing module contribute to the corresponding term in  $a_N(q)$ . Hence, the necessary condition imposes differential diffusion. Again, if there are coefficients of higher degree, they further restrict the space of parameters compatible with Turing instability.

To illustrate the principle for the relaxation of diffusion constraints, one node of a minimal topology at a time is assumed to be immobile to obtain a Turing network of different Type according to the diffusion constraints. The same procedure is applied in SM4 to 4-node and non-minimal networks to demonstrate the power of the graph-based framework to analyze the relaxation of diffusion constraints in complex networks. The CIMA reaction [7, 9] and the relaxation principle operating in several models from the literature [14, 15, 17, 13] are also analyzed in SM5. The topology shown 2 has all nodes diffusible and therefore can only produce Type-I Turing networks. If the subgraph induced by  $u$  and  $v$  is the destabilizing module and  $v$  is assumed to be immobile, the coefficient

$a_3(q)$  given in eq.8 is reduced to:

$$a_3(q) = a_3(0) - q^2 \overset{\uparrow}{\underset{u}{\downarrow}} \cdot \overset{\uparrow}{\underset{vw}{\downarrow}} - q^2 \overset{\uparrow}{\underset{w}{\downarrow}} \cdot \overset{\uparrow}{\underset{uv}{\downarrow}} \quad (11)$$

Hence, the network is still a Type-I Turing system limited by the constraint given in eq.10: the diffusion rate of  $w$  must be bigger than that of  $u$ , otherwise the coefficient of degree  $q^2$  cannot be negative. If this occurs, the sufficient condition  $a_3(q)$  is fulfilled automatically for sufficiently large wavenumbers. Conversely the same topology becomes a Type-II network assuming that  $w$  is immobile and that the subgraph induced by  $w$  and  $v$  is the destabilizing module. Then, the coefficient  $a_3(q)$  is:

$$a_3(q) = a_3(0) - q^2 \overset{\uparrow}{\underset{u}{\downarrow}} \cdot \overset{\uparrow}{\underset{vw}{\downarrow}} - q^4 \overset{\uparrow}{\underset{u}{\downarrow}} \overset{\uparrow}{\underset{v}{\downarrow}} \cdot \odot \quad (12)$$

Thus, the destabilizing module is the only contributing term to the coefficient of degree 2 in  $a_3(q)$  and the necessary condition that stems from Descartes' rule is fulfilled automatically and independently of the diffusion ratio  $d$ . Because there is a coefficient of larger degree in  $q$ , fulfillment of the sufficient condition  $a_3(q) < 0$  involves the diffusion ratio, but as expected from a Type-II network, it can be satisfied with  $d = 1$ .

Finally, the topology from 2 is transformed into a Type-III network assuming that the subgraph induced by  $u$  and  $v$  is the destabilizing module and that  $u$  is not diffusible. In this case, the destabilizing module is the only contributor to the leading coefficient in  $a_3(q)$ :

$$a_3(q) = a_3(0) - q^2 \overset{\uparrow}{\underset{w}{\downarrow}} \cdot \overset{\uparrow}{\underset{uv}{\downarrow}} \quad (13)$$

Thus, the topology guarantees the fulfillment of both the necessary *and* the sufficient conditions for the existence of Turing patterns, independently of the diffusion rates. Understanding the topological mechanism that underlies the relaxation of diffusion constraints facilitates the design of Turing networks. Relaxation occurs if at least one stabilizing  $\ell_R$ -subgraph of the same size than the destabilizing module has at least one complementary node that is immobile. The immobile node necessarily belongs to the destabilizing module, since its complementary nodes must all be diffusible. It follows that making non-diffusible a node that is complementary to several stabilizing cycles is an efficient way to relax the diffusion constraints. Likewise, as more nodes of the destabilizing module are assumed to be immobile, it is more likely that subgraphs of the network lose their stabilizing influence and that the diffusion constraints are weakened. This is the reason why in larger networks, which can have larger destabilizing modules that accommodate more immobile nodes, the fraction of Type-II and Type-III networks increases. Thus, the graph-based analysis makes the explanation of this observation straightforward.

## Turing filters and Oscillatory Turing networks

The extreme case of Turing networks in which all nodes of the destabilizing module are immobile deserves special attention. We previously discovered that

these networks are all Type-III and their dynamic behavior is qualitatively different from standard Turing networks: the wavelength of the emergent pattern is not determined by the network but by the external perturbation [18].

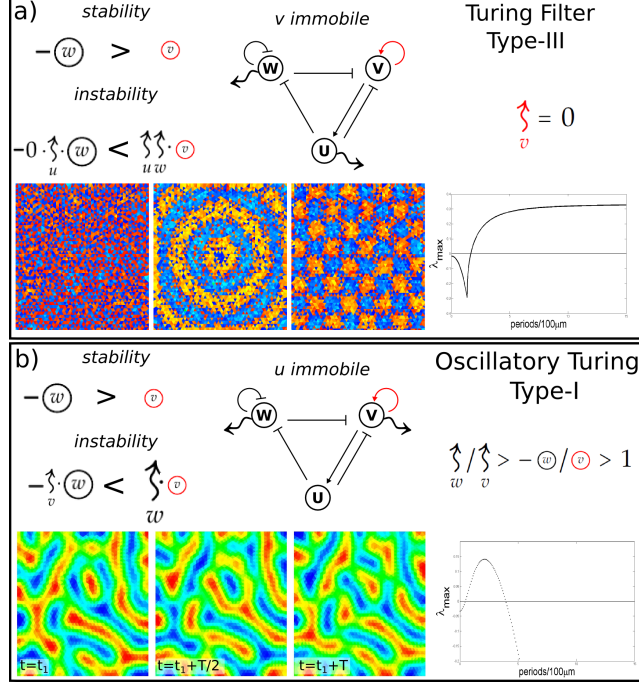


Figure 4: Minimal topology with 1 immobile node becomes a) Turing filter. The destabilizing module formed by an immobile node. The dispersion relationship saturates to a maximum value for infinitely small wavelengths: in the presence of noise it amplifies noise, but it can also amplify pre-patterns of wavelength smaller than critical value b) Oscillatory network of Type-I. The dotted dispersion relationship indicates a complex eigenvalue.

The reason is that the dispersion relationship does not have a peak that determines the pattern wavelength. Instead, the maximum eigenvalue grows monotonically from a negative value at  $q = 0$  and tends asymptotically to a maximum positive value for large wave-numbers. The formal proof of this result is given in SM6 using Rouché's theorem. Thus, modes with a wavenumber below the critical value are not amplified, whereas modes with a larger wavenumber grow with comparable speeds. Therefore, the emergent patterns do not have a characteristic wavelength determined by the network. Instead, the initial perturbation that kicks the system out of the homogeneous equilibrium is what determines the pattern that emerges. If the initial perturbation has a spatial structure with a wavelength smaller than the critical value, the system amplifies it to form a stationary pattern with the same spatial structure. Conversely, an initial pre-pattern with wavelength above the critical value is not amplified. If the homogeneous state is driven out of equilibrium by a small amplitude white

noise, all the modes present in the perturbation grow. In this scenario, the modes that grow faster are those with infinitely small wavelength, and for this reason the system evolves to form a stationary salt-and-pepper pattern. In this sense, this subset of Type-III networks are not genuine spontaneous pattern forming systems and they could rather be called Turing filters.

The results obtained so far have focused on stationary Turing patterns. However, the analysis can be extended to oscillatory Turing patterns with only minor modifications. Indeed, the classification according to diffusion constraints and the topological arrangements that distinguish the different Types carries over for most networks generating oscillatory Turing patterns. These are the networks in which the instability occurs when a coefficient  $a_{k < N}(q)$  turns negative, while  $a_N(q)$  remains positive. Hence, the subgraph that causes the instability spans  $k < N$  nodes. An important difference is that the conditions for the existence of oscillatory Turing patterns are sufficient but not necessary. This means that not all networks capable of generating oscillatory Turing patterns are covered. The networks left out of the analysis are however rare and are subject to severe constraints in their kinetic parameters although, interestingly, they can be built without any positive cycle and do not require differential diffusivity (see SM1 for details). Oscillatory Turing filters also exist and like their stationary counterparts are characterized by having a destabilizing module composed of non-diffusible nodes. They have less patterning power than Stationary Turing filters: noisy perturbation inputs or stochastic dynamics combined with oscillations destroy any pre-pattern and evolve to form an oscillating salt-and-pepper pattern of large amplitude. However, if the system is assumed to follow deterministic dynamics, the amplification of input perturbations with a characteristic wavelength that falls in the flat region of the dispersion relationship is comparable to the amplification of salt-and-pepper patterns. In this instance, Oscillatory Turing filters can produce a pattern that results from the oscillatory coupling of several modes and rich dynamics ensue.

## Topology and Robustness

A common criticism about Turing systems is that they are not robust, because small parameter variations impair their patterning potential. This feature is related to what has been referred as the fine-tuning problem, noting that Turing systems require either unrealistic separation of diffusion scales or unphysical fine-tuning of kinetic parameters [6]. Generally, it is not known what determines the size of the parameter space of a Turing system. Murray investigated the robustness of several 2-node Turing models and found large variations in the size of their Turing space [26]. Several biologically motivated models have shown that the size of the parameter space of receptor-ligand based Turing systems massively increases when the diffusion of the receptor is restricted to single cells [14, 27] or is assumed to be immobile [15, 17]. Previously, we made a computational screen to find all minimal Turing networks of 3 and 4 nodes with two diffusible species [18]. The calculation of the size of the parameter space of these networks revealed a trade-off between stability and instability conditions. These observations can be partially understood in the framework of our theory. All minimal Turing networks of a given number of nodes can be grouped into a limited number of topological families. A topological family has a unique and minimal distribution of cycles that allows to build networks that can be stable

without diffusion and that can undergo diffusion-driven instabilities.

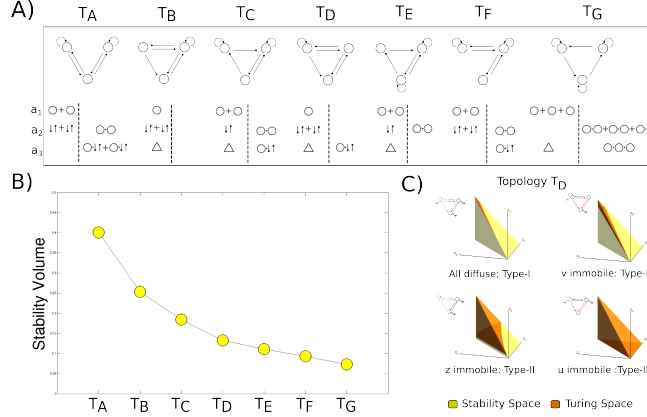


Figure 5: a) Seven topological families contain all 3-node Turing networks. Unique distribution of cycles and  $\ell_R$ -subgraphs is shown below. b) Stability space of 3-node topological families. The Stability space for all Turing networks within a family is invariant c) Comparison of the Turing space for  $T_D$  networks when all nodes diffuse (top-left, fine-tuning necessary) or one of the nodes is immobile (rest, fine-tuning not required) with  $d = 1.5$  in all cases.

For example, the 21 non-isomorphic Turing networks of 3 nodes found in our previous computational screen [18] can be grouped into just 7 topological families shown in 5a. Similarly, we found 64 non-isomorphic Turing networks of 4 nodes that can be classified into just 12 topological families, which are shown in SM10. A conjecture about the relationship between the number of nodes and edges required to build a minimal Turing topology and other relevant properties are also discussed in SM10. Crucially, all networks that belong to the same topological family have an identical Stability space. Furthermore, the size of the Stability space of different topological families varies markedly, as shown in 5b. The reason is that the Stability space is formed by the intersection of the hypersurfaces defined by the Routh-Hurwitz stability conditions. Importantly, these conditions depend only on the network cycles and  $\ell_R$ -subgraphs that they form. Because of this, and restricting the analysis to systems in which the interactions between species do not depend on the steady state, the Stability space is determined exclusively by the topological family of the network. In turn, the Turing space is the fraction of the Stability space that is compatible with diffusion-driven instabilities and is determined by the diffusion rates. Precisely, the key variable is the ratio between the diffusion rates of the nodes that induce the destabilizing module and its complementary nodes. If all nodes diffuse, the Turing space tends to zero as this ratio tends to one. This is precisely the source of the fine-tuning problem: if realistic differences in diffusion rates are assumed, the size Turing space becomes infinitesimal. The fundamental cause of this behavior is the opposite requirements of stability without diffusion and the condition stemming from Decartes' rule necessary for Turing instabilities. These two requirements can be combined in a particularly simple form if the destabilizing module  $\ell^{ins}$  does not overlap with the other stabilizing subgraphs

of the same size  $(\ell_1^{st}, \dots, \ell_m^{st})$ :

$$d^{N-k} > \frac{|\ell_1^{st}| + \dots + |\ell_m^{st}|}{|\ell^{ins}|} > 1 \quad (14)$$

where  $d$  is the ratio between the diffusion of nodes complementary to the destabilizing module and the nodes that induce it, and  $k$  is the size of the destabilizing module. Note that as  $d$  tends to 1 the space of parameters that can fulfill both inequalities vanishes. However, as demonstrated before, this behavior depends on the assumption that all nodes diffuse. If there are nodes in the destabilizing module that are immobile, the second inequality does not apply and networks of different Type according to the diffusion constraints can be obtained. Even if all the nodes that diffuse do so at the same rate, the Turing space does not vanish, as shown in 5c for a particular topological family. Thus, the robustness of a Turing network results from a combination of two factors: i) the topological family, which determines the volume of the Stability space and ii) the Type given by which nodes are immobile, which determines the Turing space. This illustrates the power of analyzing Turing systems through a topological lens, since it shows that the fine-tuning problem is not intrinsic to Turing systems, it reveals its source, and how to bypass it.

## 2.2 Topology and Pattern Phases

The original 2-node network postulated by Turing can be implemented in two different forms, typically referred to as activator-inhibitor and substrate-depleted models [28]. The activator-inhibitor network forms a periodic pattern in which the concentrations of the two species are in-phase, whereas in the substrate-depleted they are out-of-phase. Both networks have the same topology: a node with a positive loop and a node with a negative loop connected by negative cycle of length 2, but with the signs of the edges flipped. Thus, the two networks have the same distribution of cycles and cycle signs but differ in the signs of their edges, which leads to the difference in patterns. For both networks, the analytic expression of the conditions for Turing instability and the dispersion relationship are identical [29], so that the wavelength and speed of growth of the patterns generated are also identical, provided that the kinetic parameters have the same absolute values. The analysis of Turing networks through the graph-theoretical lens shows how these properties carry over for networks of any number of nodes.

First, networks that have the same topology and the same distribution of cycle signs are restricted to identical requirements for the existence of diffusion-driven instabilities and generate patterns with the same wave-length and growing speed. The reason for this is that the conditions for stability without diffusion and for Turing instability depend exclusively on  $\ell$ -subgraphs and cycles, rather than individual kinetic parameters. Thus, kinetic parameters and diffusion rates are subjected to the same restrictions for the existence of Turing patterns. For the same reason, the dispersion relationship emerging from the solution of the linearization problem 2 is identical for networks with the same topology and cycle sign distribution, so that the dynamics and wavelength of the pattern that they generate are the same.

Second,  $N$  species can be grouped in two phases in exactly  $2^{N-1}$  different ways. This is therefore the number of different Turing patterns that  $N$  species

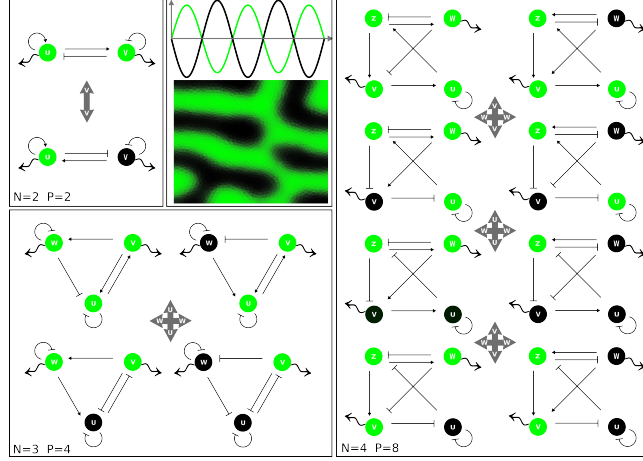


Figure 6: There are  $2^{N-1}$  ways to group  $N$  species in a *green* and a *black* phase of Turing pattern. A topology allows to construct  $2^{N-1}$  different Turing networks with the sign of the cycles invariant. Each network makes one of the patterns. Grey arrows indicate the node to which the sign of outgoing and ingoing edges has been switched, producing a change in phase.

could hypothetically form. For example, a 3-node network can form  $4 = 2^{3-1}$  patterns: 1 pattern with all species in phase and 3 patterns with one of the species being out-of-phase with the rest. A 4-node network can form  $8 = 2^{4-1}$  patterns: 1 with all species in phase, 4 with one species being out-of-phase with the rest and 3 with a pair of the species out-phase with the other pair. The general combinatorial proof is given in SM7. The central finding is that each of these  $2^{N-1}$  patterns is produced by one of the  $2^{N-1}$  Turing networks that share the same topology and cycle signs but differ in the sign of individual edges. Given a network that produces a pattern with a certain distribution of species amongst the two phases, it is possible to construct the network that produces the same pattern but with a single species switched to the other phase by flipping the signs of all the edges coming in and out of the corresponding node. Note that this transformation leaves invariant the sign of all the cycles passing through the node, including the loops. Applying the same transformation to several nodes at a time, the associated species switch to the opposite phase. There are exactly  $2^{N-1}$  different networks that can be constructed in this way, each generating one of the  $2^{N-1}$  possible Turing patterns. The formal proof in terms of similarity transformations of the Jacobian of the reaction-diffusion equations is given in SM7. Intuitively, it can be understood that the effect of switching the signs of the edges going in and out of a node is equivalent to inverting the concentration of this node.

In addition, we find that examination of the topology of a minimal network also allows to predict the phases of the reactants. Typically, this is done by calculating numerically the eigenvectors of the linearized system for a particular choice of parameter values. Conversely, the method based on examining the topology (detailed in SM8) is independent of parameter values and provides an intuitive understanding of Turing dynamics.

### 3 Discussion

In real world systems it is easier to obtain reliable information about the topology of a reaction network than precise quantitative values of the parameters such as reaction rates or diffusion constants. This is especially so in biology, because these parameters are generally estimated from in vitro experiments, and yet the real effective values in vivo are likely to be quite different. Consequently, a theory which allows us to determine properties of a Turing system from its topology ideally complements quantitative measurements to obtain novel insights into patterning systems. In this work we show that central properties of a Turing system can indeed be understood purely through the analysis of its topology. First, we tackle the question of the requirements of differential diffusion, and in which ways these requirements can be relaxed. A commonly discussed method of relaxing diffusion constraints has been the concept of hindered diffusion through the introduction of an immobile node [7]. This has been well known since the discovery of the CIMA reaction, but corresponds to a very specific topological change - the immobile node reversibly binds a self-activating node in such a way that it effectively slows down the diffusion and is inert to the rest of the network. Beyond the original CIMA reaction, this idea has also been implicated in biological systems in which receptors bound to the cell membrane or the extracellular matrix play the role of an immobile node that reduces the diffusion of a ligand [30]. However, we discovered that there exist alternative ways to achieve similar and even greater relaxation of constraints [18], which do not correspond to the notion of hindered diffusion. The present theory provides a complete understanding of the relationship between topology and diffusion constraints, and the general principle for their relaxation. Indeed, this principle is general in the sense that it explains the relaxation of diffusion constraints in networks of any size or number of diffusible nodes. We show that the CIMA reaction and models with the same architecture are networks of Type-II, so the relaxation of the constraints is not maximized. Other designs, such as Type III circuits, are not working by hindered diffusion, and yet allow far more robust systems. Furthermore, understanding the principle of relaxation allows us to identify designs that could be optimal for experimental implementation of Turing patterns in chemical or synthetic biosystems. For example, in SM4 we show how to construct a 4-node Type-III network with just one immobile node. Crucially, these types of networks do not suffer the fine-tuning problem, a common criticism of the plausibility of Turing patterns in real biological systems [5]. Finally, we addressed the question of which patterns can be generated by a Turing system, and in particular, which phase relationships the molecules will have with respect to each other. We showed here that inverting the sign of the interactions of a node with the rest of the network has the effect of switching its phase in the pattern. This operation can be performed sequentially on any node of the circuit, in this way generating all possible phase combinations of the nodes of the system - irrespective of how many nodes there are.

In summary, our theory explains the relationship between topology and three fundamental properties of Turing systems. Our findings should help to finally dispel important objections that have been made against the role of Turing patterns in biological development. They will also be very powerful for the inference of circuits underlying real biological patterns, and will be of practical use in the race for the design of the first synthetic Turing biosystem [31].



## References

- [1] Alan Mathison Turing. The chemical basis of morphogenesis. *Philosophical Transactions of the Royal Society of London B: Biological Sciences*, 237(641):37–72, 1952.
- [2] Vincent Castets, Etienne Dulos, Jacques Boissonade, and Patrick De Kepper. Experimental evidence of a sustained standing turing-type nonequilibrium chemical pattern. *Physical Review Letters*, 64(24):2953–2956, 1990.
- [3] Qi Ouyang and Harry L Swinney. Transition from a uniform state to hexagonal and striped turing patterns. *Nature*, 352(6336):610–612, 1991.
- [4] J. D. Murray. *Mathematical Biology II*. Springer, 3rd edition, January 2003.
- [5] Ruth E Baker, EA Gaffney, and PK Maini. Partial differential equations for self-organization in cellular and developmental biology. *Nonlinearity*, 21(11):R251, 2008.
- [6] Thomas Butler and Nigel Goldenfeld. Fluctuation-driven turing patterns. *Physical Review E*, 84(1):011112, 2011.
- [7] Istvan Lengyel and Irving R Epstein. Modeling of turing structures in the chloriteiodidemalonic acidstarch reaction system. *Science*, 251(4994):650–652, 1991.
- [8] K Agladze, E Dulos, and P De Kepper. Turing patterns in confined gel and gel-free media. *The Journal of Physical Chemistry*, 96(6):2400–2403, 1992.
- [9] Istvan Lengyel and Irving R Epstein. A chemical approach to designing turing patterns in reaction-diffusion systems. *Proceedings of the National Academy of Sciences*, 89(9):3977–3979, 1992.
- [10] Judit Horvth, Istvn Szalai, and Patrick De Kepper. An experimental design method leading to chemical turing patterns. *Science*, 324(5928):772–775, 2009.
- [11] Istvn Szalai, Judit Horvth, and Patrick De Kepper. Contribution to an effective design method for stationary reaction-diffusion patterns. *Chaos: An Interdisciplinary Journal of Nonlinear Science*, 25(6):064311, 2015.
- [12] John E Pearson. Pattern formation in a (2+ 1)-species activator-inhibitor-immobilizer system. *Physica A: Statistical Mechanics and its Applications*, 188(1):178–189, 1992.
- [13] K Korvasov, EA Gaffney, PK Maini, MA Ferreira, and V Klika. Investigating the turing conditions for diffusion-driven instability in the presence of a binding immobile substrate. *Journal of theoretical biology*, 367:286–295, 2015.

- [14] Erik M Rauch and Mark M Millonas. The role of trans-membrane signal transduction in turing-type cellular pattern formation. *Journal of theoretical biology*, 226(4):401–407, 2004.
- [15] Herbert Levine and Wouter-Jan Rappel. Membrane-bound turing patterns. *Physical Review E*, 72(6):061912, 2005.
- [16] Damin E Strier and Silvina Ponce Dawson. Turing patterns inside cells. *PLoS One*, 2(10):e1053–, 2007.
- [17] Vclav Klika, Ruth E Baker, Denis Headon, and Eamonn A Gaffney. The influence of receptor-mediated interactions on reaction-diffusion mechanisms of cellular self-organisation. *Bulletin of mathematical biology*, 74(4):935–957, 2012.
- [18] Luciano Marcon, Xavier Diego, James Sharpe, and Patrick Mller. High-throughput mathematical analysis identifies turing networks for patterning with equally diffusing signals. *eLife*, 5:e14022, 2016.
- [19] R. G. Casten and C. J. Holland. Stability properties of solutions to systems of reaction-diffusion equations. *SIAM Journal on Applied Mathematics*, 33(2):353–364, September 1977.
- [20] F.R. Gantmacher. *Applications Of The Theory Of Matrices*. Interscience Publishers, 1959.
- [21] Bruce L Clarke and Weimin Jiang. Method for deriving hopf and saddle-node bifurcation hypersurfaces and application to a model of the belousov-zhabotinskii system. *The Journal of chemical physics*, 99(6):4464–4478, 1993.
- [22] Maya Mincheva and Marc R Roussel. Graph-theoretic methods for the analysis of chemical and biochemical networks. i. multistability and oscillations in ordinary differential equation models. *Journal of mathematical biology*, 55(1):61., 2007.
- [23] R.A. Brualdi and D. Cvetkovic. *A Combinatorial Approach to Matrix Theory and Its Applications*. Chapman and Hall/CRC, 2008.
- [24] R.A. Horn and C. R. Johnson. *Matrix Analysis*. Cambridge University Press, February 1990.
- [25] Dirk Jan Struik. *A source book in mathematics, 1200-1800*. Princeton University Press, 2014.
- [26] JD Murray. Parameter space for turing instability in reaction diffusion mechanisms: a comparison of models. *Journal of Theoretical Biology*, 98(1):143–163, 1982.
- [27] Tams Kurics, Denis Menshykau, and Dagmar Iber. Feedback, receptor clustering, and receptor restriction to single cells yield large turing spaces for ligand-receptor-based turing models. *Physical Review E*, 90(2):022716, 2014.

- [28] Alfred Gierer and Hans Meinhardt. A theory of biological pattern formation. *Biological Cybernetics*, 12(1):30–39, 1972.
- [29] Takashi Miura and Philip K Maini. Speed of pattern appearance in reaction-diffusion models: implications in the pattern formation of limb bud mesenchyme cells. *Bulletin of mathematical biology*, 66(4):627–649, 2004.
- [30] Patrick Müller, Katherine W Rogers, R Yu Shuizi, Michael Brand, and Alexander F Schier. Morphogen transport. *Development*, 140(8):1621–1638, 2013.
- [31] Natalie S Scholes and Mark Isalan. A three-step framework for programming pattern formation. *Current Opinion in Chemical Biology*, 40:1–7, 2017.

# Supplementary Material for Key features of Turing systems are determined purely by network topology

Xavier Diego<sup>a,b</sup>, Luciano Marcon<sup>c</sup>, Patrick Müller<sup>c</sup>, and James Sharpe<sup>a,b,d</sup>

<sup>a</sup> EMBL-CRG Systems Biology Research Unit, Center for Genomic Regulation, Barcelona Institute for Science and Technology, Barcelona, Spain

<sup>b</sup> Universitat Pompeu Fabra, Barcelona, Spain

<sup>c</sup> Friedrich Miescher Laboratory of the Max Planck Society, Germany

<sup>d</sup> Institutio Catalana de Recerca i Estudis Avancats, Barcelona, Spain

## Contents

<b>1</b>	<b>Conditions for stationary and oscillatory Turing patterns</b>	<b>2</b>
<b>2</b>	<b>Coates graph of a reaction-diffusion system and <math>\ell</math>-subgraphs examples</b>	<b>4</b>
<b>3</b>	<b>Necessity of a destabilizing module for stationary Turing patterns</b>	<b>7</b>
<b>4</b>	<b>Examples of relaxation of diffusion constraints</b>	<b>9</b>
4.1	A 4-node minimal network . . . . .	9
4.2	The complete 3-node network . . . . .	11
4.3	A 4-node network of Type-III with just one immobile node . . .	13
<b>5</b>	<b>Analysis of the relaxation of diffusion constraints in Turing models from the literature</b>	<b>14</b>
5.1	The CIMA reaction . . . . .	14
5.2	Turing models from the literature . . . . .	16
5.2.1	Models based on the CIMA architecture . . . . .	16
5.2.2	Hair follicle formation . . . . .	18
<b>6</b>	<b>Turing filters and Rouché's Theorem</b>	<b>19</b>
<b>7</b>	<b>Properties of Turing pattern phases</b>	<b>21</b>
<b>8</b>	<b>Rule of thumb to predict pattern phases</b>	<b>23</b>
<b>9</b>	<b>Algebraic proof of the impossibility of Turing patterns in systems with all species diffusing at the same rate</b>	<b>25</b>

<b>10 On Turing minimal networks</b>	<b>25</b>
10.1 Conjecture about number of edges of minimal network . . . . .	25
10.2 Turing topological families of 4 nodes . . . . .	27

## 1 Conditions for stationary and oscillatory Turing patterns

The necessary and sufficient conditions for all the roots of a polynomial to lie in the left half of the complex plane are given by the Routh-Hurwitz criterion [1, see Chapter 6]. For a polynomial  $P(\lambda) = \lambda^N + a_1\lambda^{N-1} + \dots + a_N$ , the Hurwitz matrix is defined in terms of its coefficients as:

$$H = \begin{bmatrix} a_1 & a_0 & 0 & 0 & \dots & 0 \\ a_3 & a_2 & a_1 & a_0 & \dots & 0 \\ a_5 & a_4 & a_3 & a_2 & \dots & 0 \\ \vdots & \vdots & \vdots & \vdots & \dots & \vdots \\ \vdots & \vdots & \vdots & \vdots & \ddots & \vdots \\ 0 & 0 & 0 & 0 & 0 & a_N \end{bmatrix} \quad (1)$$

The Routh-Hurwitz criterion states that all roots of the polynomial have negative real parts if and only if

$$\Delta_j = \det[H(j)] > 0 \quad j = 1, \dots, N \quad (2)$$

where  $H(j)$  is the submatrix obtained by taking the first  $j$  rows and columns of the Hurwitz matrix. A polynomial that fulfills these conditions is said to be stable. If the conditions are not fulfilled, the number of roots with positive real part is given by the number of sign changes in the Routh array [1, pag 230]:

$$R = [1, \Delta_1, \frac{\Delta_2}{\Delta_1}, \frac{\Delta_3}{\Delta_2}, \dots, \frac{\Delta_N}{\Delta_{N-1}}] \quad (3)$$

where the last entry of the Routh array can be simplified to  $\Delta_N/\Delta_{N-1} = a_N$ . A corollary of Routh-Hurwitz criterion is that the positivity of all the  $a_k$  coefficients is a necessary condition for stability.

$$a_k > 0 \quad k = 1, \dots, N \quad (4)$$

Conversely, if any of the coefficients is negative there exists at least one root with positive real part and the polynomial is unstable. Hence,  $a_k < 0$  for some  $k$  is a sufficient condition for the instability of a polynomial.

This theorem allows to derive the conditions for the existence of diffusion-driven instabilities in a reaction-diffusion system because they are determined by the zeroes of the characteristic polynomial defined as:

$$P_q(\lambda) = \det[\lambda \mathbf{I} - \mathbf{F}^{\text{RD}}(q)] = \lambda^N + a_1(q)\lambda^{N-1} + \dots + a_N(q) \quad (5)$$

where  $\mathbf{F}^{\text{RD}}(q) = \mathbf{J}^{\text{R}}(r_o) - q^2 \mathbf{D}$  has been defined in the main text. The system is assumed to be stable in the absence of diffusion. This means that for  $q = 0$  all the eigenvalues of  $P_q(\lambda)$  are in the left half of the complex plane. Diffusion-driven instability occurs because  $P_q(\lambda)$  loses stability when at least one eigenvalue crosses to the right half of the complex plane for  $q > 0$ . Note that  $P_q(\lambda)$  is a

real polynomial and its complex eigenvalues always occur in conjugate pairs. Stationary Turing patterns occur when a single, real eigenvalue becomes positive and are associated with a saddle-node bifurcation. Oscillatory patterns, in turn, occur when a single pair of complex conjugate eigenvalues crosses to the right half of the complex plane and are associated with a Hopf bifurcation. Next we will show that examination of the signs of  $a_k(q)$  can allow to determine the type of bifurcation that has occurred.

If a single real eigenvalue of  $P_q(\lambda)$  crosses to the right half of the complex plane, then it is necessary that  $a_N(q) < 0$  for some  $q > 0$ . This follows from the identity:

$$a_N(q) = \det[-\mathbf{F}^{\text{RD}}(q)] = (-1)^N (\lambda_1 \cdot \dots \cdot \lambda_N) \quad (6)$$

A sufficient condition would require ruling out that other eigenvalues cross to the right hand of the complex plane simultaneously. This can be enforced if the rest of the Hurwitz determinants are positive<sup>1</sup>, so that the sign pattern of the Hurwitz array is  $R = [+ , + , \dots , + , -]$ . However, a necessary condition for stationary patterns is enough for the purposes of investigating diffusion constraints in Turing systems, which is the focus of this work.

A pair of complex eigenvalues crosses to the right half of the complex plane, without a real eigenvalue turning positive simultaneously, if and only if  $a_N(q) > 0$  while  $\Delta_{N-1}(q) = 0$  for some range  $q > 0$ . The first condition guarantees that there are no real eigenvalues crossing to the right half of the complex plane, and the second condition stems from Orlando's formula [1, 2]:

$$\Delta_{N-1} = (-1)^{N \cdot (N-1)/2} \prod_{i < k} (\lambda_i + \lambda_k) \quad (7)$$

Deriving analytical conditions from the Hurwitz determinant is impractical even for moderately sized networks. The condition derived in [3] that there exists  $a_{k < N}(q) < 0$  for  $q > 0$  while  $a_N(q) > 0$ , is simpler but it is only sufficient. This means that it can not identify all oscillatory Turing networks. Particularly, networks associated to a Hurwitz determinant turning negative while the coefficients  $a_k$  remain positive are not detected, as remarked in the main text. This behavior occurs if for example  $a_1(q) \cdot a_2(q) < a_3(q)$ . Thus, the kinetic parameters are typically subjected to severe nonlinear constraints, but interestingly, these networks do not require a destabilizing module or differential diffusivity.

---

<sup>1</sup>More complex dynamics can occur when real and complex eigenvalues with positive real parts coexist. Ruling this out requires analyzing all the Hurwitz determinants, and this becomes rapidly intractable even for networks of moderate size. The simplified conditions  $a_k(q) > 0$  for  $k < N$  and  $a_N(q) < 0$  guarantee that a single real eigenvalue turns positive, but they can not exclude that a complex pair does as well. For networks of size  $N \leq 3$ , these simplified conditions are sufficient to guarantee that only a real eigenvalue turns positive, since in this case  $\Delta_1 = a_1(q) > 0$  and  $\Delta_2 = a_1(q)a_2(q) - a_3(q) > 0$ . For minimal networks of size  $N \leq 5$ , we observe that in most cases they also result in a simple stationary Turing instability. This is possibly due to the dominance of the diagonal terms  $\Delta_i = a_1 \cdot a_2 \cdot \dots \cdot a_i$  over the off-diagonal terms in the Hurwitz determinants [2], which is more pronounced in minimal networks. This precludes instabilities associated to Hurwitz determinants of order smaller than  $N$  turning negative while  $a_k(q) > 0$  for  $k < N$ . For non-minimal networks, however, the existence of pairs of complex eigenvalues has to be ruled out on a case by case basis.

## 2 Coates graph of a reaction-diffusion system and $\ell$ -subgraphs examples

The reaction-diffusion graph of a reaction-diffusion system has been introduced to illuminate the relationship between topology and fundamental properties of a Turing systems. The key element is to associate a weighted digraph to the matrix  $\mathbf{F}^{\text{RD}}$  obtained from the linear approximation of the reaction-diffusion equations. The reaction-diffusion graph will be denoted as  $G[\mathbf{F}^{\text{RD}}]$ . Similarly, a graph can be associated only to the jacobian of the reaction term and will be denoted as  $G[\mathbf{J}^{\text{R}}]$ . The definition of the reaction-diffusion graph is based on the definition of the Coates Graph of a matrix, whose introduction has been attributed to C.L. Coates [4]. An extensive introduction to this formalism can be found in Brualdi's book [5]. A detailed explanation of the application of this theoretical framework to the analysis of reaction-diffusion systems was given in [6]. In this section we provide a summary of the essential results and examples of  $\ell$ -subgraphs. The reaction-diffusion graph of a general 4 node network is shown in SM fig.1 to illustrate the definitions given in the main text.

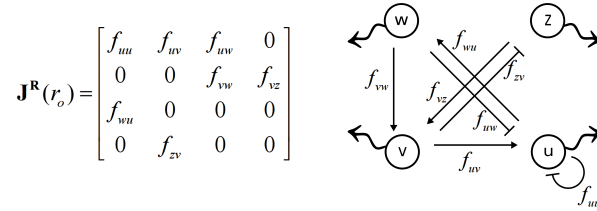


Figure 1: Reaction-diffusion graph of a minimal 4-node network associated to  $\mathbf{F}^{\text{RD}}(q) = \mathbf{J}^{\text{R}}(r_o) - q^2\mathbf{D}$ . All species are assumed to diffuse.

Intuitively, the subgraph induced by a subset of nodes is the subgraph formed by these nodes and the edges between them. According to this definition, the subgraph  $I_{\gamma_k}$  induced by the nodes  $\gamma_k = (i_1, i_2, \dots, i_k)$  corresponds the Coates graph  $G[\mathbf{F}_{\gamma_k}^{\text{RD}}]$ , where  $\mathbf{F}_{\gamma_k}^{\text{RD}}$  is the submatrix formed by row and column indices in  $\gamma_k$ . In this way we can establish a one-to-one correspondence between each principal submatrix  $\mathbf{F}_{\gamma_k}^{\text{RD}}$  and an Induced subgraph  $I_{\gamma_k}$ . Examples of this correspondence for two Induced Subgraphs of the previous network are shown in SM fig.2:

There are  $\binom{N}{k}$  different  $k$ -by- $k$  principal submatrices in a  $N$ -by- $N$  matrix. The coefficient  $a_k(q)$  of the characteristic polynomial  $P_q(\lambda)$  defined in eq. 5 can be obtained from the sum of the signed determinants of all the  $k$ -by- $k$  principal submatrices [7]:

$$a_k(q) = \sum_{\gamma_k} (-1)^k \det[\mathbf{F}_{\gamma_k}^{\text{RD}}(q)] \quad (8)$$

The Coates formula provides a graphical interpretation of the determinant of a matrix. Precisely, the signed determinant of a  $k$ -by- $k$  matrix  $\mathbf{F}_{\gamma_k}^{\text{RD}}$  is given by the sum of the weights of all  $\ell$ -subgraphs contained in the Induced subgraph  $I_{\gamma_k}$ .

$$(-1)^k \det[\mathbf{F}_{\gamma_k}^{\text{RD}}(q)] = \sum_{\ell \subseteq I_{\gamma_k}} w(\ell) \quad (9)$$

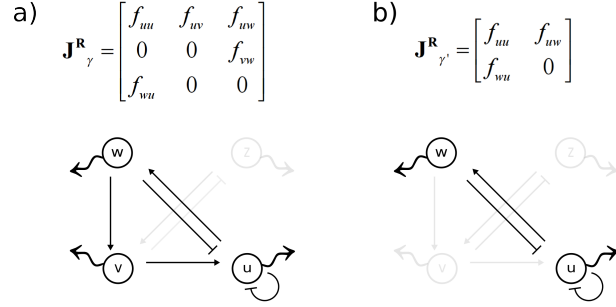


Figure 2: a) Induced Subgraph of size 3 induced by  $\gamma = (u, v, w)$ . b) Induced Subgraph of size 2 induced by  $\gamma' = (u, w)$ .

where the weight of an  $\ell$ -subgraph, as defined in the main text, is given by the product of the cycles that it contains and a minus sign for every cycle. Thus, introducing this expression in eq. 9 we can express  $a_k(q)$  as a sum over the  $\ell$ -subgraphs of size  $k$ . The example network from SM fig.1 contains 4 cycles that are shown next:

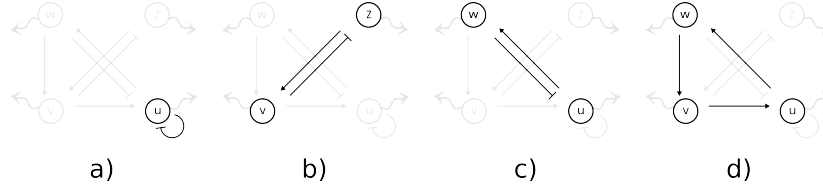


Figure 3: The network from SM fig.1 contains a) one reaction cycle of size 1 b) and c) two reaction cycles of size 2 and d) one reaction cycle of size 3.

Non-overlapping combinations of these cycles form the  $\ell_R$ -subgraphs that determine the stability of the network without considering diffusion. In turn, combinations of these cycles and diffusive loops form the  $\ell_{RD}$ -subgraphs that determine the patterning dynamics. SM fig.4 depicts the  $\ell$ -subgraphs contained in the examples of Induced Subgraphs shown previously, and SM fig.5 shows the  $\ell$ -subgraphs that span all the nodes in the network.



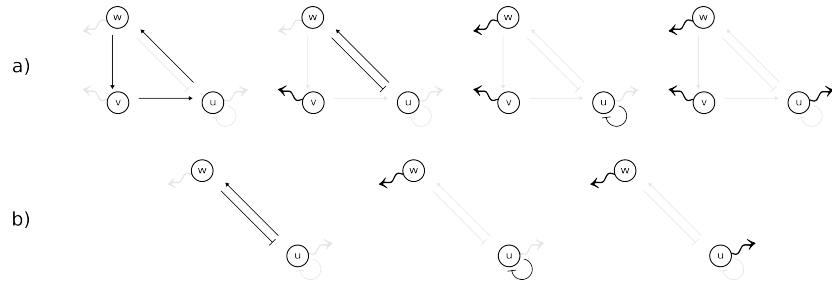


Figure 4: a)  $I_{\gamma=(u,v,w)}$  contains, from left to right: an  $\ell_R$ -subgraph formed by a cycle of length 3,  $\ell_{RD}$ -subgraph formed by a cycle of length 2 and a diffusive loop,  $\ell_{RD}$ -subgraph formed by a reaction loop and two diffusive loops, an  $\ell_D$ -subgraph formed by 3 diffusive loops. b)  $I_{\gamma'=(u,w)}$  contains an  $\ell_R$ -subgraph formed by a cycle of length 2, an  $\ell_{RD}$ -subgraph formed by a diffusive and a reaction loop, an  $\ell_D$ -subgraph formed by two diffusive loops.

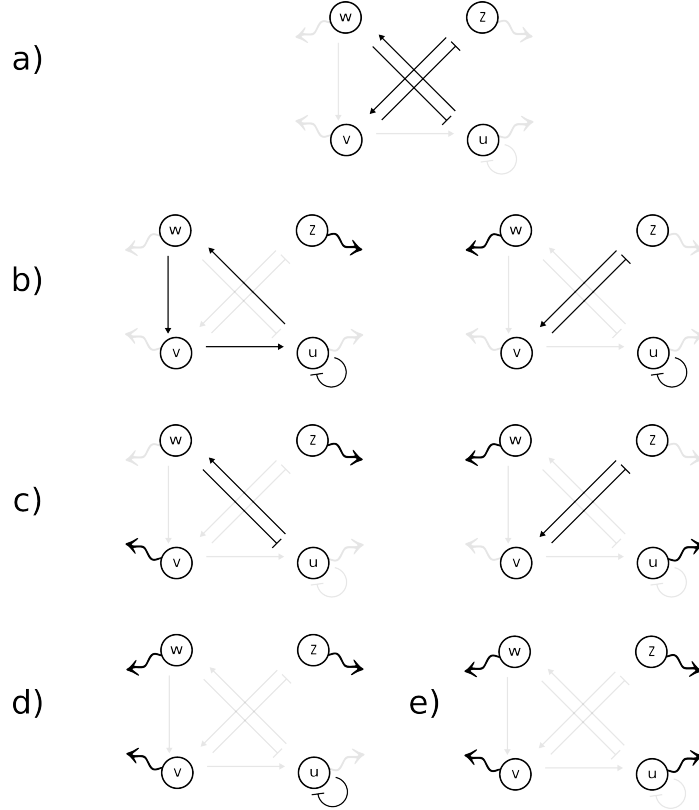


Figure 5:  $\ell$ -subgraphs of size 4 contained in the network from SM fig.1 are ordered in rows according to the number of diffusive loops contained.

### 3 Necessity of a destabilizing module for stationary Turing patterns

A destabilizing module of a reaction-diffusion system has been defined as an Induced Subgraph of  $G[\mathbf{J}^{\mathbf{R}}(r_o)]$  in which the destabilizing  $\ell_R$ -subgraphs outweigh the stabilizing  $\ell_R$ -subgraphs. In the main text we state that a Turing system that generates stationary patterns must have a destabilizing module of smaller size than the size of the full system. The necessary condition of having a destabilizing module is related to a condition based on the property of matrix  $s$ -stability investigated in [8] and the minor condition investigated in [9]. These results can both be derived from the relationship between  $P_0$ -matrices and strong stability proved earlier by Cross in [10, Theorems 1-2] or a similar result by Othmer [11]. Here we provide an alternative proof that is more direct and clarifies the reason why a destabilizing module (and therefore a positive cycle) are necessary for stationary Turing patterns but not for oscillatory Turing patterns. We also provide the interpretation of this result in terms of the reaction-diffusion graph.

**Theorem** *A destabilizing module in a reaction-diffusion system is a necessary condition for the existence of stationary Turing patterns.*

*Proof:* Let  $\mathbf{A}$  be a real  $N \times N$  matrix and  $\mathbf{A}_{\gamma_k}$  denote its  $k$ -by- $k$  principal submatrix formed by the entries with rows and column indices given by  $\gamma_k = (i_1, \dots, i_k)$ .

**Definition** The matrix  $\mathbf{A}$  is said to be a  $P_0$ -matrix if all the signed principal minors are nonnegative:

$$(-1)^k \det[\mathbf{A}_{\gamma_k}] \geq 0 \quad \forall \gamma_k \quad k = 1, \dots, N \quad (10)$$

The subset  $P_0^+$  is formed by the  $P_0$ -matrices that have at least one positive signed minor of each order for  $k = 1, \dots, N$ . The eigenvalues of a  $P_0$ -matrix are excluded from a wedge around the positive half of the real axis, as proved by Kellogg in [12, theorem 4]. Let  $\lambda = r \exp(i\theta)$  be an eigenvalue of a  $N \times N$   $P_0$ -matrix, where  $\theta$  is the polar angle measured from the positive real axis<sup>2</sup>. Then:

**Theorem** [Kellogg]  $\lambda = r \exp(i\theta)$  is an eigenvalue of a  $N \times N$   $P_0$ -matrix if and only if  $|\theta| \geq \pi/N$

Another result, proved by Cross in [10, Proposition 1, pag. 257], shows that the region of eigenvalue exclusion of a  $P_0$ -matrix  $\mathbf{A}$  also applies to  $\mathbf{A} - \mathbf{D}$ , where  $\mathbf{D}$  is a nonnegative diagonal matrix:

**Theorem** [Cross] If a matrix  $\mathbf{A} \in P_0$  or  $\mathbf{A} \in P_0^+$ , the same is true of  $\mathbf{A} - \mathbf{D}$  for all  $\mathbf{D} \geq 0$ .

---

<sup>2</sup>The definitions used in Kellogg's paper [12] differ from those adopted here, which follow the definitions given in Cross paper [10]. The difference lays in a minus sign in the definition of a  $P$ ,  $P_0$  and  $P_0^+$ -matrices. The adaptation of the results to the alternative convention is straightforward, using the following property of the spectrum of a matrix  $\sigma(-\mathbf{A}) = -\sigma(\mathbf{A})$

The relevance of this result for the existence of stationary diffusion-driven instabilities is straightforward. Provided that  $\mathbf{J}(r_o)$  is a  $P_0$ -matrix, the eigenvalues of  $\mathbf{J}(r_o) - q^2 \mathbf{D}$  cannot cross to the positive half of the complex plane along the real axis, and stationary Turing pattern can not occur. It follows that is necessary that  $\mathbf{J}(r_o)$  is not a  $P_o$ -matrix.

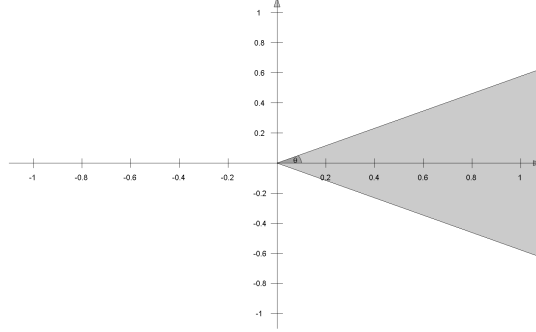


Figure 6: The exclusion region for the eigenvalues of a  $P_0$ -matrix  $\mathbf{A}$  and  $\mathbf{A} - q^2 \mathbf{D}$  are the same.  $N = 6$ ,  $\theta = 30^\circ$

Note that a  $P_0$ -matrix can have a pair of complex eigenvalues that cross to the right half of the complex plane with  $q > 0$ . Hence,  $\mathbf{J}^{\mathbf{R}}(r_o) \notin P_o$  is not necessary for oscillatory Turing patterns. This explains the counterexample found in [13] to a conjecture given in [9] that proposes that  $P_0$ -matrices are strongly stable. This result holds for  $N \leq 3$  but is not true in general, as was already discussed by Cross in [10]. These type of oscillatory networks are not covered by our theory: the instability is produced when a Hurwitz determinant  $\Delta_{j < N}$  changes sign while all the coefficients  $a_K(q)$  remain positive. Thus, these type of networks can undergo diffusion-driven instabilities without having a positive cycle or destabilizing module. However, they seem to be restricted to severe parametric requirements.

We now proceed to examine the graphical implications of the necessary condition for stationary Turing patterns. That  $\mathbf{J}^{\mathbf{R}}(r_o)$  is not a  $P_o$ -matrix implies that there is a principal submatrix of  $\mathbf{J}^{\mathbf{R}}(r_o)$  whose signed minor is negative. Since  $\mathbf{J}^{\mathbf{R}}(r_o)$  is stable, the size of the submatrix is  $k < N$ . This submatrix can be associated to the subgraph of  $G[\mathbf{J}^{\mathbf{R}}(r_o)]$  induced by a set of nodes  $\gamma_k = (i_1, \dots, i_k)$ . Further, the value of the signed principal minor is equal to the weight of the associated induced subgraph, which is in turn given by the weights of all the  $\ell$ -subgraphs contained in it:

$$(-1)^k \det[\mathbf{J}^{\mathbf{R}}(r_o)_{\gamma_k}] = w(I_{\gamma_k}) = \sum_{\ell \subseteq I_{\gamma_k}} w(\ell) < 0 \quad (11)$$

Therefore, there is an Induced subgraph of size smaller than  $N$  in which the destabilizing  $\ell$ -subgraphs outweigh the stabilizing  $\ell$ -subgraph, which completes the proof.

## 4 Examples of relaxation of diffusion constraints

Several networks will be analyzed to illustrate the relaxation of diffusion constraints. The first is a 4-node network, this will show how the graph-based analysis is not hampered by an increase in the number of nodes. The second is a general 3-node Turing network, this will show that the same is true for non-minimal networks. The third is a another 4-node minimal network that, interestingly, becomes a Type-III network with just one diffusible node. This makes it an ideal design to engineer a system that can generate Turing patterns.

### 4.1 A 4-node minimal network

The 4-node network analyzed was shown in SM fig.1. The destabilizing module is the subgraph induced by node  $\gamma = (u, v, w)$  that contains a positive cycle of length 3. First we will assume that all nodes are diffusible, then we will set one node at a time as non-diffusible, and finally we will set two nodes as immobile nodes to obtain a Type-III network.

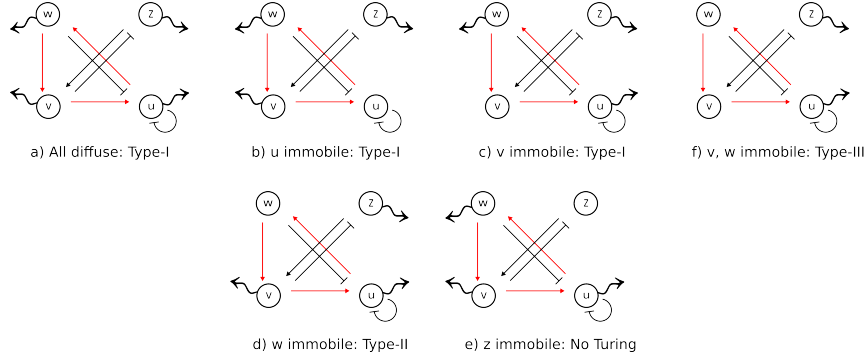


Figure 7: Different degrees of relaxation of the diffusion constraints are achieved by assuming that different nodes are immobile

#### a) All nodes diffuse: Type-I network

If all nodes are diffusible, the network is necessarily a Type-I Turing network, as demonstrated in the main text. The explicit form of the constraints is readily obtain examining  $a_3(0)$  and  $a_4(q)$ . The coefficient  $a_3(0)$  must be positive for the network to be stable. Conversely,  $a_4(q) > 0$  for some  $q > 0$  is required for diffusion-driven instability:

$$a_3(0) = -\frac{\Delta_{uvw}}{uvv} + \frac{\Theta_{vz}}{vz} > 0$$

$$a_4(q) = +\frac{\Uparrow_{vz}}{vz} \cdot \frac{\Uparrow_{uw}}{uw} + q^2 \left( -\frac{\Delta_{uvw}}{uvw} \cdot \frac{\Updownarrow_z}{z} + \frac{\Theta_{vz}}{vz} \cdot \frac{\Updownarrow_w}{w} \right) + q^4 \left( -\frac{\Uparrow_{uw}}{uw} \cdot \frac{\Updownarrow_{vz}}{vz} - \frac{\Uparrow_{vz}}{vz} \cdot \frac{\Updownarrow_{uw}}{uw} \right) - \frac{\Theta_{vwz}}{vwz} \cdot q^6 + \frac{\Theta_{uvwz}}{uvwz} \cdot q^8 < 0$$

The nested structure of the polynomial makes necessary that  $\Updownarrow_z > \Updownarrow_w$  so that the term of order  $q^2$  can be negative and the condition stemming from Decartes rule is fulfilled. Hence, the network is of Type-I.

**b)  $u$  immobile: Type-I network**

Setting the diffusion rate of a node to zero does not affect the  $\ell_R$ -subgraphs formed purely by reaction cycles. Hence,  $a_3(0)$  is not changed. Conversely,  $a_4(q)$  becomes:

$$a_4(q) = + \underset{vz}{\uparrow\downarrow} \cdot \underset{uw}{\uparrow\downarrow} + q^2(- \underset{uvw}{\triangle} \cdot \underset{z}{\uparrow} + \underset{vz}{\oplus} \cdot \underset{w}{\uparrow\downarrow} \cdot \underset{z}{\uparrow}) + q^4(- \underset{uw}{\uparrow\downarrow} \cdot \underset{vz}{\uparrow\downarrow} \cdot \underset{z}{\uparrow\downarrow}) - \underset{vwz}{\oplus} \cdot q^6 \underset{vwz}{\uparrow\downarrow\uparrow\downarrow\uparrow\downarrow} < 0$$

The condition  $\uparrow_z > \uparrow_w$  is still required to make the term of order  $q^2$  negative. The network requires differential diffusivity and is therefore a Type-I network. The topological reason that explains why this occurs is that the immobile node  $u$  is not complementary to  $\underset{vz}{\oplus} \cdot \uparrow\downarrow$ , the stabilizing  $\ell$ -subgraph of the same size than the destabilizing module.

However, setting the node  $u$  immobile is not ineffectual: it results in the disappearance of stabilizing terms of order  $q^4$  and  $q^8$ . This, in turn, facilitates the fulfillment of the condition  $a_4(q) < 0$  and weakens the requirements on the kinetic parameters. For this reason, this network has a larger Turing space than the case with all nodes diffusing.

**c)  $v$  immobile: Type-I network**

In this case,  $a_4(q)$  and the condition for Turing instability are:

$$a_4(q) = + \underset{vz}{\uparrow\downarrow} \cdot \underset{uw}{\uparrow\downarrow} + q^2(- \underset{uvw}{\triangle} \cdot \underset{z}{\uparrow} + \underset{vz}{\oplus} \cdot \underset{w}{\uparrow\downarrow} \cdot \underset{z}{\uparrow}) + q^4(- \underset{vz}{\uparrow\downarrow} \cdot \underset{uw}{\uparrow\downarrow} \cdot \underset{z}{\uparrow\downarrow}) < 0$$

As in the previous case, the immobile node is not complementary to the stabilizing  $\ell$ -subgraph of the same size than the destabilizing module. Turing instability requires  $\uparrow_z > \uparrow_w$  and the network is of Type-I. The disappearance of more stabilizing terms of higher order implies that this network is even more robust than the previous case.

**d)  $w$  immobile: Type-II network**

In this case,  $a_4(q)$  and the condition for Turing instability are:

$$a_4(q) = + \underset{vz}{\uparrow\downarrow} \cdot \underset{uw}{\uparrow\downarrow} + q^2(- \underset{uvw}{\triangle} \cdot \underset{z}{\uparrow}) + q^4(- \underset{uw}{\uparrow\downarrow} \cdot \underset{vz}{\uparrow\downarrow} \cdot \underset{z}{\uparrow\downarrow}) < 0$$

The stabilizing  $\ell$ -subgraph of the same size than the destabilizing module vanishes. Hence, differential diffusivity is no longer required to fulfill the condition stemming from Decartes' rule. However, the condition  $a_4(q) < 0$  still involves the diffusion rates, and therefore they are not completely unconstrained. The network is then of Type-II. The explicit form of the constraint is:

$$\frac{\uparrow_z}{\uparrow_v} > - \frac{4 \cdot \underset{vz}{\uparrow\downarrow} \cdot \underset{uv}{\uparrow\downarrow}^2}{\underset{uvw}{\triangle}^2} \quad (12)$$

Note that this inequality can be fulfilled even if  $\uparrow_z = \uparrow_w$  by setting the appropriate values of the 3 cycles involved in the constraint. An additional degree of freedom is furnished by the cycle that is not involved in the inequality. Typically, this results in a larger Turing space than in Type-I networks.

**e)  $z$  immobile: Network cannot produce Turing patterns**

In this case,  $a_4(q)$  and the condition for Turing instability are:

$$a_4(q) = + \underset{vz}{\uparrow\downarrow} \cdot \underset{uw}{\uparrow\downarrow} + q^2 (+ \underset{vw}{\oplus} \cdot \underset{zw}{\uparrow\downarrow} \cdot \underset{uw}{\uparrow\downarrow}) + q^4 (- \underset{vz}{\uparrow\downarrow} \cdot \underset{uw}{\uparrow\downarrow} \cdot \underset{vw}{\uparrow\downarrow} \cdot \underset{zw}{\uparrow\downarrow}) < 0$$

This inequality cannot be fulfilled, since there is no negative term in  $a_4(q)$ . The destabilizing influence of  $\Delta_{uvw}$  is lost because its complementary node is immobile. This is true in general: if there are nodes complementary to the destabilizing module that are immobile the network cannot undergo stationary Turing instability.

**f)  $w, z$  immobile: Type-III network**

If these two nodes are assumed to be immobile,  $a_4(q)$  and the condition for Turing instability are:

$$a_4(q) = + \underset{vz}{\uparrow\downarrow} \cdot \underset{uw}{\uparrow\downarrow} + q^2 (- \underset{uvw}{\Delta} \cdot \underset{z}{\uparrow\downarrow}) < 0$$

The inequality is fulfilled independently of the values of the diffusion rate of  $u$  and  $z$ , because the destabilizing module is the only contributor to the leading term in  $q^2$ . Thus, the network is of Type-III and the Turing volume is equal to the Stability volume.

## 4.2 The complete 3-node network

A 3-node network with all possible interactions between its nodes is shown in SM fig.8. The destabilizing module is assumed to be induced by  $u$  and  $v$ .

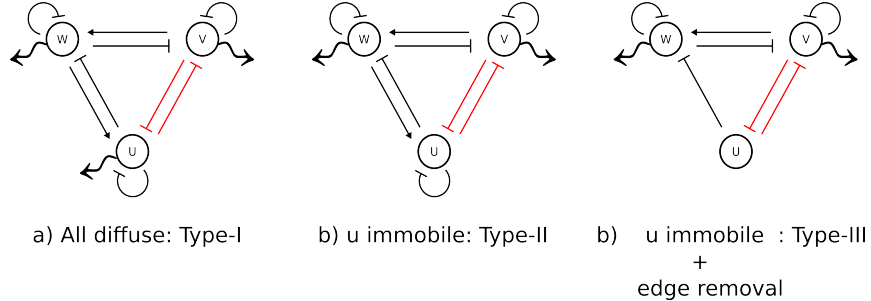


Figure 8: Relaxation of the diffusion constraints in a non-minimal 3N network.

a) All nodes diffuse: Type-I

The coefficient  $a_2(0)$  and  $a_3(q)$  of the complete  $3N$  network are:

[illegible]

Assuming for simplicity that the diffusion rates of  $u$  and  $v$  are equal, the constraints stemming from stability and Descartes' rule on the diffusion ratio  $d = \zeta_w / \zeta_u = \zeta_w / \zeta_v$  can be combined in the following form:

$$d > \frac{\frac{(\textcircled{u}\textcircled{w}) - \uparrow\downarrow}{uw} + \frac{(\textcircled{v}\textcircled{w}) - \uparrow\downarrow}{vw}}{-\frac{(\textcircled{u}\textcircled{v}) - \textcolor{red}{\uparrow\downarrow}}{uv}} > 1 \quad (13)$$

Thus, the complete 3-node network with all nodes diffusing is a Type-I network<sup>3</sup>.

**b)  $u$  or  $v$  immobile: Type-II**

The complete 3-node network is transformed into a Type-II network by assuming that either of the two nodes that induce the destabilizing module is immobile. For example, assuming that  $u$  is immobile,  $a_2(0)$  does not change but  $a_3(q)$  becomes:

$$a_3(q) = a_3(0) + q^2 \underbrace{\uparrow \downarrow}_{w} (\textcircled{u} \textcircled{v}) - \underbrace{\uparrow \downarrow}_{wv} + q^2 \underbrace{\uparrow \downarrow}_v (\textcircled{u} \textcircled{w}) - \underbrace{\uparrow \downarrow}_{vw} \\ - q^4 \underbrace{\uparrow \downarrow \uparrow \downarrow}_{vw} (\textcircled{u})$$

In this case, the conditions stemming from Descartes' rule is fulfilled provided that

$$d > \frac{(\textcircled{u} \textcircled{w} - \textcircled{\uparrow \downarrow})_{uw}}{-(\textcircled{u} \textcircled{v} - \textcircled{\uparrow \downarrow})_{uv}} \quad (14)$$

Note that the diffusion ratio is not unconstrained, but since the expression on the right hand side does not need to be bigger than 1, the two diffusible molecules can diffuse at the same rate.

c)  $u$  immobile, removal of 2 edges: Type-III

To obtain a Type-III network is necessary that the destabilizing module is the  $\ell_R$ -subgraph of smaller order that contributes to  $a_N(q)$ . In this way the destabilizing module forms the leading term in  $a_N(q)$ . The modifications required

<sup>3</sup>Alternatively, if  $\textcircled{u}$  were the destabilizing cycle in the network, then the coefficient of degree  $q^4$  in  $a_3(q)$  could be negative. Imposing this and that  $a_1(0) > 0$  and defining the diffusion ratio as before  $d$  as before leads to the analogous constraint  $d > -(\textcircled{v} + \textcircled{u})/\textcircled{u} > 1$ . As expected, the constraint of a Type-I network is recovered.

to achieve this are easily deduced observing equation 4.2. Thus, removing the loop  $\odot$  and one of the edges from  $\updownarrow_{uw}$  the coefficient  $a_3(q)$  becomes:

$$a_3(q) = a_3(0) - q^2 \updownarrow_w \cdot \updownarrow_{uv}$$

Thus, diffusion-driven instabilities occur independently of the diffusion rates of the diffusible molecules.

### 4.3 A 4-node network of Type-III with just one immobile node

The network shown in SM fig.9 is necessarily a Type-I network when all nodes are diffusing. The nested structure of the polynomial is the source of the differential diffusivity requirement, since the  $q^2$  and  $q^4$  can only become negative if the diffusion rates of the nodes that form the destabilizing module are smaller than the complementary nodes. This can be appreciated in the expression of stability conditions  $a_2(0) > 0$  and  $a_3(0) > 0$  and the diffusion-driven instability condition  $a_4(q) < 0$ :

$$\begin{aligned} a_2(0) &= -\updownarrow_{vz} - \updownarrow_{uv} > 0 \\ a_3(0) &= -\triangle_{vzw} + \odot_u \cdot \updownarrow_{vz} > 0 \\ a_4(q) &= \triangle_{vzw} \cdot \odot_u - q^2 \updownarrow_u \cdot \triangle_{vwz} + q^2 \updownarrow_w \cdot \odot_u \cdot \updownarrow_{vz} - q^4 \updownarrow_{uw} \cdot \updownarrow_{vz} - q^4 \updownarrow_{wz} \cdot \updownarrow_{uv} \\ &\quad - q^6 \updownarrow_{vwz} \cdot \odot_u - q^8 \updownarrow_{uvwz} < 0 \end{aligned}$$

This network is particularly interesting because the destabilizing module is of size two, which allows to transform it into a Type-III network by assuming that just one nodes, in this case  $z$ , is immobile.

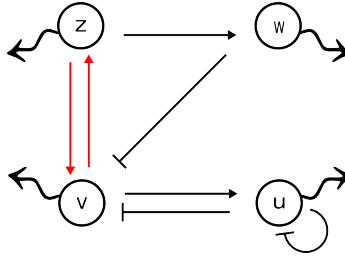


Figure 9: Network that becomes a Type-III assuming  $z$  is immobile

The reason is that this change removes the stabilizing effect of all the subgraphs of the same *and* smaller size than the destabilizing module. Hence, the destabilizing module becomes to only contributor to the leading term in  $a_4(q)$ :

$$a_4(q) = \triangle_{vzw} \cdot \odot_u - q^2 \updownarrow_u \cdot \triangle_{vwz} + q^2 \updownarrow_w \cdot \odot_u \cdot \updownarrow_{vz} - q^4 \updownarrow_{uw} \cdot \updownarrow_{vz}$$



Note that this behavior would not be possible if the destabilizing module were of size 3; in this case the cycles of smaller size typically forms a stabilizing term of higher order in  $q$  than the destabilizing module. A topology with a positive cycle of size two in turn requires that there is another cycle of size two to confer stability. Thus, such an efficient weakening of the diffusion constrains with single immobile node is permitted by very specific topological features. In fact, there are just two  $4N$  topological families, listed as  $T_B$  and  $T_J$  in SM fig.19, in which this behavior is possible. The second topological family, however, generates Oscillatory Turing networks for the sets of parameter values, as  $a_3(q)$  also turns negative.

Topology  $T_B$  is attractive for the purpose of designing a Turing system experimentally: it has a small number of edges (minimal in fact), a simple mutual activation cycle (easier to engineer than a positive cycle of size 3, be it in a series of chemical reactions or recycling and modifying existing signaling pathways in a cell) and just one immobile species (in a chemical system this is desirable because diffusible reactants should be the norm rather than the exception and in a biological system this means that just one transcription factor would be involved). More importantly, the fact that it is a Type-III network means that the range of values of the kinetic constants that fulfill the Turing conditions is very large. Particularly, this design should have a larger Turing space than designs that follow the CIMA architecture [14, 15].

## 5 Analysis of the relaxation of diffusion constraints in Turing models from the literature

### 5.1 The CIMA reaction

The Chlorite-Iodide-Malonic Acid-starch reaction (CIMA) reaction was the system in which stationary Turing patterns were first observed [16]. Lengyel and Epstein analyzed a model that correctly describes the temporal behavior of the reaction to investigate the patterning mechanism underlying the reaction [17]. This analysis suggested that starch, introduced as an indicator to visualize the formation of spatial structures, forms a complex with iodine that cannot diffuse in the gel where the reaction occurred. In this way, the effective diffusion of the activator (iodine,  $I^-$ ) is reduced, producing the difference in diffusion with the inhibitor (chlorite,  $ClO_2^-$ ) that is required for Turing instabilities. By making a series of reasonable approximations about the underlying chemical processes, the description of the CIMA reaction can be reduced to a 3-species reaction-diffusion model [14]. Writing the concentration of the activator as  $[I^-] = u$ , the inhibitor  $[ClO_2^-] = v$ , starch as  $s_0$  and the starch-iodine complex  $[SI_3^-] = su$ , the Lengyel-Epstein model is:

$$\begin{aligned}\frac{\partial u}{\partial t} &= f(u, v) - k_+ s_o \cdot u + k_- \cdot su + D_u \frac{\partial^2 u}{\partial x^2} \\ \frac{\partial v}{\partial t} &= g(u, v) + D_v \frac{\partial^2 v}{\partial x^2} \\ \frac{\partial su}{\partial t} &= k_+ s_o \cdot u - k_- \cdot su\end{aligned}\tag{15}$$

The kinetic constants  $k_+$  and  $k_-$  give the rates of formation and dissociation of the starch-iodine complex. Lengyel and Epstein further simplified the analysis by assuming that the formation and dissociation of the complex is very fast. With this approximation, the concentration of the complex is given by  $sx = (k_+ \cdot s_0 / k_-)u$  because it is in instantaneous equilibrium with the activator  $u$ . The CIMA model is then simplified to a set of two reaction-diffusion equations for  $u$  and  $v$  and, importantly, this transformation introduces a timescale separation between the two species that reflects that the activator is being trapped and released by the starch in the medium. Using realistic values for the parameters in the model, Lengyel and Epstein estimated that without starch the diffusion rate of  $v$  ought to be 10 times faster than that of  $u$  to generate Turing instabilities. According to the Stokes-Einstein law, the diffusion of two ions of similar sizes in aqueous solution cannot possibly be that different. However, the introduction of starch reduces the necessary ratio of diffusion rates to a more plausible value of 1.5.

Next we use our graph-based formalism to analyze the mechanism of relation of diffusion constraints in the CIMA reaction. The analysis does not require the assumption of fast complex formation and in this respect is more general. The reaction-diffusion graph associated to the Lengyel-Epstein model of the CIMA reaction given by eq.15 is obtained following the procedure detailed in the main text and shown in 10.

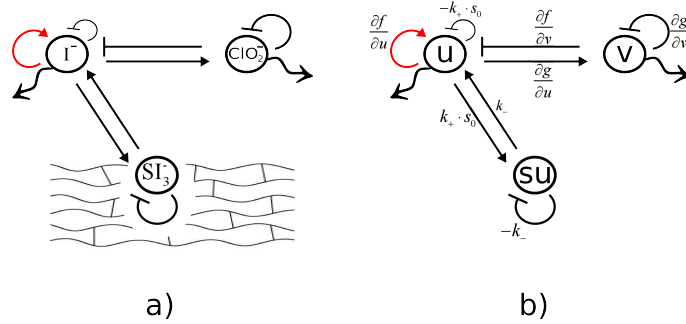


Figure 10: The CIMA model (a) by Lengyel and Epstein[14] and associated reaction-diffusion graph (b). Iodine  $I^-$  acts as the activator, chlorite  $ClO_2^-$  as the inhibitor and the starch-iodine complex  $SI_3^-$  cannot diffuse.

The activator has two loops that correspond to the self-activation term  $\partial f / \partial u$  and the term  $k_+ \cdot s_0$  that gives the rate of decrease in concentration of  $u$  through complex formation. In graph notation this is represented by  $\odot u = \odot u_a + \odot u_c$ , with the first loop accounting for self-activation and the second for complex formation. In addition, the edges that form the cycle between  $u$  and  $su$  and their loops are not independent because the number of iodide molecules is conserved and therefore  $\uparrow_{u \cdot su} = -\odot u_c \cdot -\odot u_c$ . These identities lead to following simplification of the subgraph induced by  $u$  and  $su$ :

$$\begin{aligned}
(\textcircled{u} \textcircled{v} - \textcircled{u} \textcircled{v})_{u \cdot s u} &= [(\textcircled{u_a} + \textcircled{u_c}) \textcircled{v} - (-\textcircled{u_c} \cdot -\textcircled{v})] \\
&= \textcircled{u_a} \textcircled{v}
\end{aligned}$$

In turn, this simplifies the coefficient  $a_3$  of the characteristic polynomial to:

$$\begin{aligned}
a_3(q) &= a_3(0) + q^2 [\textcircled{v} \textcircled{u} \textcircled{v}]_u + (\textcircled{u} \textcircled{v} - \textcircled{u} \textcircled{v})_{u \cdot s u} \textcircled{v} - q^4 \textcircled{u} \textcircled{v} \textcircled{u} \textcircled{v} \\
&= a_3(0) + q^2 [\textcircled{v} \textcircled{u} \textcircled{v}]_u + \textcircled{u_a} \textcircled{v} \textcircled{v} - q^4 \textcircled{u} \textcircled{v} \textcircled{u} \textcircled{v}
\end{aligned}$$

Hence, the only term in  $a_3(q)$  that can be negative in order to fulfill the necessary condition for stationary Turing patterns is the coefficient of  $q^2$ . The form of  $a_3(q)$  is characteristic of a Type-II Turing system according to the diffusion constrains. Indeed, defining  $d = \textcircled{v} / \textcircled{u}$ , this condition can be expressed as:

$$d > -\frac{\textcircled{v}}{\textcircled{u_a}}$$

Importantly, stability requirements do not impose that  $\textcircled{u_a}$  is smaller than  $\textcircled{v}$ , because the network contains other stabilizing loops:

$$a_1(0) = -(\textcircled{v} + \textcircled{u_a} + \textcircled{u_c} + \textcircled{v}) > 0 \not\Rightarrow \textcircled{u_a} < -\textcircled{v}$$

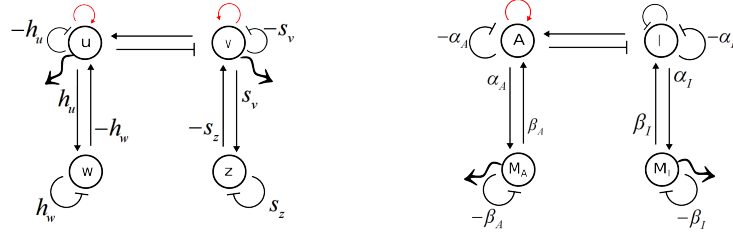
Hence, the diffusion ratio can be equal to 1 and even smaller, depending on the parameter values of  $\textcircled{u_a}$  and  $\textcircled{v}$ . The explicit form of the constraints for the kinetic parameters can be obtained examining the rest of the stability conditions  $a_i(0) > 0$ , but they do not further limit the diffusion ratio of the activator and the inhibitor. Thus, this analysis allows us to easily derive the diffusion constraints of the CIMA reaction and does not require the approximation that complex formation is very fast. Importantly, all networks designs based on the CIMA architecture result in a Type-II Turing system, due to the existence of stabilizing terms involving more diffusion loops. Examples of such networks can be found in [18, 19, 20].

## 5.2 Turing models from the literature

### 5.2.1 Models based on the CIMA architecture

In this section we analyze two Turing models inspired by the CIMA reaction. The first is a recent investigation of the conditions for diffusion-driven instability in the presence of binding immobile substrates by Korvasova and collaborators [20]. This is a purely theoretical study that aimed to weaken the restrictive conditions that apply to diffusion rates and kinetic parameters of 2-node Turing networks. To that end, they analyzed the Lengyel-Epstein model [14] of the CIMA reaction using standard linear stability analysis and algebraic manipulations. They also proposed a 4-node generalization of the CIMA model in which two self-activators bind two immobile substrates. The corresponding reaction-diffusion graph is shown in SM fig.11a. The principle behind the re-

laxation of diffusion constraints is the same than in the CIMA reaction. The transient bonds between activator and substrates do not change the number



a) Korvasova (2015): Type-II

b) Rauch (2004): Type-II

Figure 11: a) Network composed of diffusable activators  $u$  and  $v$  that bind to immobile substrates [20] b) A model of biological patterning based on morphogens  $M_A$  and  $M_I$  that diffuse in the extracellular space and gene products that are confined inside cells [18]

of molecules. As in the CIMA model, the subgraphs induced by these pairs simplify to  $\odot \odot - \updownarrow = \odot \odot$  and  $\odot \odot - \updownarrow = \odot \odot$ , where the loop notation makes explicit the contribution from self-interaction and complex formation as in the CIMA reaction. The Turing condition  $a_4(q) < 0$  can then be expressed as:

$$\begin{aligned}
 a_4(q) &= a_4(0) + q^2 [-\odot(\odot \odot - \updownarrow) - \odot(\odot \odot - \updownarrow)] + q^4 \odot \odot \odot \odot \\
 &= a_4(0) - q^2 (\odot \odot + \odot \odot) \odot \odot + q^4 \odot \odot \odot \odot
 \end{aligned}$$

The existence of two activators introduces additional relaxation of constraints compared to the original CIMA model: the necessary condition stemming from Decartes rule of signs is guaranteed because there is a term in  $a_4(q)$  formed only by destabilizing terms. However, there is a stabilizing subgraph that contains more diffusive loops and because of this the conditions for diffusion-driven instabilities are not independent of the diffusion rates. Still, as in the CIMA reaction, the diffusion rates can be equal and the network is of Type-II.

The second model to be analyzed was proposed by Rauch and collaborators [18] as plausible mechanism of biological pattern formation. The model consists of biochemical reactions between gene products that are confined inside cells and therefore can be considered non-diffusible and messenger molecules that are secreted by cells and can diffuse between them. The associated reaction-graph is shown in SM fig.11b. Taking advantage of the simplifications that follow from mass conservation as in the previous model, the  $a_4(q)$  coefficient can be expressed as:

$$a_4(q) = a_4(0) - q^2 \left[ \odot \odot (M_I(A_I I) - \updownarrow) + \odot \odot (M_A(I_A A) - \updownarrow) \right] + q^4 \odot \odot \odot \odot$$

Again, because the nodes  $A$  and  $I$  are not diffusible there are stabilizing subgraphs that vanish from the coefficient of degree  $q^2$  in  $a_4(q)$ . The structure of  $a_4(q)$  shows that this network, like CIMA, is also a Type-II. In this way the model shows how realistic physiological model can result in a Turing system that does not require differential diffusivity.

### 5.2.2 Hair follicle formation

A recent work by Klika et al. [21] investigates the influence of interactions mediated by immobile receptors in a model of hair-follicle patterning in vertebrate skin. The model was originally proposed by Mou and collaborators [22] and is based in their experimental analysis of the interactions between three key players in hair follicle patterning: a non-diffusing receptor (Edar), a connective tissue growth factor (CTGF) and Bone morphogenetic factor (BMP).

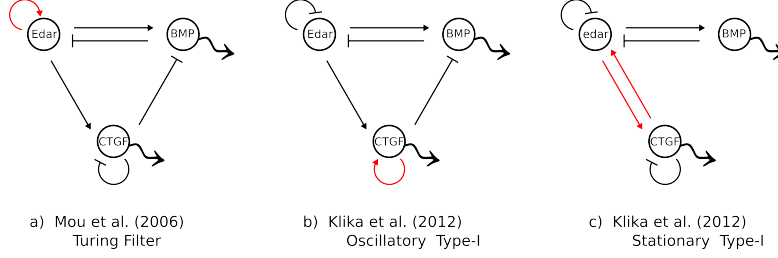


Figure 12: Three alternative models of Hair follicle patterning in proposed in [22](a) and [21] b) and c). They form a Turing Filter, a Oscillatory Turing networks of Type-I and a Stationary Turing system of Type-I respectively.

The experimental observations of Mou et al.[22] led them to propose the network shown in SM fig.12a. This network is a Turing filter. We can reach this conclusion without further analysis because the destabilizing module  $\textcircled{\text{Edar}} > 0$  is non-diffusible. The proof of the generality of this result is given in section 5. Indeed, this can be confirmed examining the form  $a_3(q)$ :

$$a_3(q) = a_3(0) + q^2 \mathcal{J}_c(\textcircled{\text{c}} \textcircled{\text{b}} - \textcircled{\text{b}}) + q^2 \mathcal{J}_{eb}(\textcircled{\text{e}} \textcircled{\text{c}} - \textcircled{\text{e}}) + q^4 \mathcal{J}_{bc} \mathcal{J}_{cb}$$

With the assumed distribution of cycle signs, the condition  $a_3(q) < 0$  for Turing instability is fulfilled independently of parameter values for  $q$  above a critical value.

Klika and collaborators [21] introduced a series of changes to the model shown in SM fig.12b due to theoretical objections. They postulated that Turing systems must be stable for very large wavenumbers. If this is not the case, they observed that infinitely small wavelengths would be amplified, generating salt-and pepper patterns for which the continuum approximation breaks down. Hence, the signs of the loops of Edar and CGTF are inverted, so that the network does not have a non-diffusible self-activator. Laborious algebraic transformation allowed them to prove that the system can not generate stationary patterns but that it can undergo oscillatory Turing instabilities.

This result is readily recovered using the graph formalism. Stability imposes that  $(\textcircled{\text{e}} \textcircled{\text{b}} - \textcircled{\text{b}}) > 0$ . This means that  $a_3(q)$  is formed only by positive terms and therefore cannot fulfill the condition  $a_3(q) < 0$ . However, the coefficient  $a_2(q)$  can fulfill  $a_2(q) < 0$ , the condition for oscillations. This requires  $\textcircled{\text{b}} > -\textcircled{\text{c}}$  and the following constraint on the diffusion ratio:

$$a_2(q) = a_2(0) - q^2 \mathcal{J}_c(\textcircled{\text{b}} + \textcircled{\text{c}}) - q^2 \mathcal{J}_b(\textcircled{\text{c}} + \textcircled{\text{e}}) + q^4 \mathcal{J}_{bc} \mathcal{J}_{cb} < 0 \Rightarrow \mathcal{J}_c \mathcal{J}_b > -\frac{(\textcircled{\text{c}} + \textcircled{\text{e}})}{(\textcircled{\text{b}} + \textcircled{\text{e}})} > 1$$

This shows that this network is a oscillatory Turing system of Type-II according to the diffusion constraints.

Finally, Klika et al. proposed an alternative network for hair-follicle patterning that is shown in SM fig.12c. The assumption behind this modification is that *CTGF* does not inhibit the production of *BMP* directly, but instead inhibits the effects of *BMP* on *Edar*. Then they showed that this network can generate stationary patterns. This result is recovered examining  $a_3(q)$ :

$$a_3(q) = a_3(0) + q^2 \underset{b}{\uparrow} (\ominus \ominus - \underset{eb}{\downarrow}) - q^2 \underset{ceb}{\uparrow} \underset{eb}{\downarrow} - \ominus \cdot q^4 \underset{bc}{\uparrow} \underset{bc}{\uparrow} < 0 \Rightarrow \underset{b}{\uparrow} / \underset{c}{\uparrow} > \frac{\underset{eb}{\uparrow}}{\ominus \ominus - \underset{eb}{\downarrow}} > 1$$

where the second inequality characteristic of Type-I networks stems from the stability condition  $a_2(0) = (\ominus \ominus - \underset{eb}{\downarrow}) - \underset{eb}{\uparrow} > 0$ .

## 6 Turing filters and Rouché's Theorem

This section demonstrates that if all the nodes of the destabilizing module are immobile the network is a Turing filter.

A Turing filter is a Type-III Turing network characterized by a dispersion relationship in which the largest eigenvalue converges asymptotically to a positive value for large wavenumbers. This means that the network does not generate patterns with a preferred wavelength, because above a certain wavenumber all eigenmodes are amplified. Further, the speed of growth of a mode increases with  $q$ . Because of this, noisy initial conditions evolve to produce a noisy pattern of large amplitude and not the typical periodic patterns of a regular Turing network. However, initial perturbations with spatial periodicity and a wavenumber above a certain threshold are amplified by these class of networks. Next we demonstrate that a Turing network with immobile nodes in the destabilizing module and diffusible nodes for the rest is a Turing filter. The proof follows the strategy used to demonstrate Theorem 1 in [10].

**Theorem.** *A network with a destabilizing module induced by immobile species generates Turing patterns independently of the values of the diffusion constants of the rest of the species. For  $q \rightarrow \infty$  the largest eigenvalue converges to the largest eigenvalue of the submatrix associated to the destabilizing module.*

*Proof:* Let the destabilizing module be a subgraph of size  $K$ . The network can be relabeled so that the nodes that induce it have indexes  $\gamma_K = (1, \dots, K)$ . The diffusion matrix is then  $\mathbf{D} = \text{diag}[0, \dots, 0, d_{K+1}, \dots, d_N]$ , where the first  $K$  entries correspond to the immobile nodes and  $d = (d_{K+1}, \dots, d_N)$  are the diffusion constants of the diffusible species. In turn, the characteristic polynomial can be written in powers of  $q$  as:

$$P_q(\lambda) = \sum_{j=0}^{N-K-1} q^{2j} \cdot b_j(\lambda, d) + q^{2(N-K)} \prod_{i=K+1}^N d_i \cdot b_{N-K}(\lambda) \quad (16)$$

For  $j < N - k$ , the coefficients  $b_j(\lambda, d_i)$  are polynomials in  $\lambda$  that depend on the diffusion constants, whereas  $b_{N-K}(\lambda) = \det[\lambda \mathbf{I} - \mathbf{J}_{\gamma_K}^R]$  is not a function of

the diffusion constants. From the identity between a matrix determinant and the product of its eigenvalues

$$\det[-J_{\gamma_K}^R] = (-1)^K \prod_{i=1}^K \lambda_i = \sum_{\ell \in I_{\gamma_K}} w(\ell) < 0 \quad (17)$$

where the last inequality uses the fact that the weight of the destabilizing module is negative. Thus, we conclude that  $J_{\gamma_K}^R$  has an eigenvalue  $\lambda_+$  with positive real part. Therefore,  $b_{N-K}(\lambda)$  has also zero at  $\lambda_+$ . Let  $C$  be a closed domain in the right half of the complex plane containing  $\lambda_+$ . For  $q$  large enough and independently of  $d_i$ , the following inequality holds in  $C$ :

$$\left| \sum_{j=0}^{N-K-1} q^{2j} \cdot b_j(\lambda, d) \right| < \left| q^{2(N-K)} \prod_{i=K+1}^N d_i \cdot b_{N-K}(\lambda) \right| \quad (18)$$

By Rouché's Theorem, this implies that  $P_q(\lambda)$  has also a zero in  $C$ , that is, an eigenvalue in the right half of the complex plane. This means that

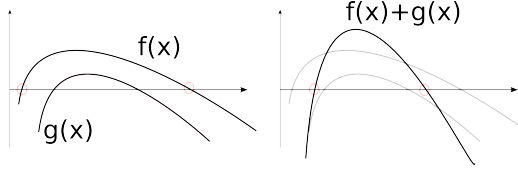


Figure 13: Rouché's theorem states that if  $f$  and  $g$  are two continuous functions in a closed domain  $C$  and  $|g(z)| < |f(z)|$  in  $C$ , then  $f$  and  $f + g$  have the same number of zeroes in  $C$ .

the network will undergo a diffusion-driven instability for wavenumbers above a certain threshold independently of the values of the diffusion constants. Further, the domain  $C$  can be made arbitrarily small around  $\lambda_+$  and for  $q$  large enough the inequality still holds. It follows that an eigenvalue of the full system converges to  $\lambda_+$  for  $q \rightarrow \infty$  and concludes the proof. To illustrate this result, the variation

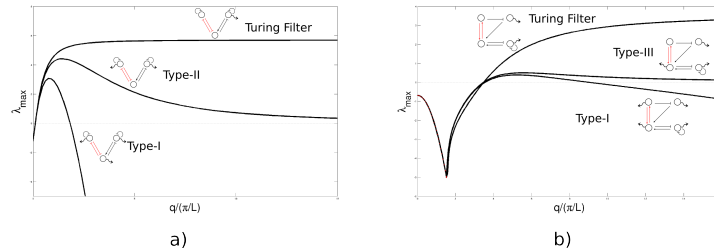


Figure 14: Dispersion relationships of two example Turing networks with all nodes diffusible, one node in the destabilizing module immobile and all the nodes in the destabilizing module immobile. The latter case produces Turing filters.

in the dispersion relationships of two Turing network as more nodes of the destabilizing module are assumed to be immobile are shown in SM fig.14.

## 7 Properties of Turing pattern phases

First we will proof that the number of Turing patterns that can be formed with  $N$  species is  $2^{N-1}$ . This simply requires counting the number of different ways in which  $N$  species can be separated in two phases.

Thus, we have to count the patterns with  $N$  species in one phase and 0 in the other (i.e.,  $\binom{N}{0} = 1$ ), with  $N-1$  species in one phase and 1 species in the other (i.e.,  $\binom{N}{1} = N$ ), with  $N-2$  species in one phase and 2 species in the other (i.e.,  $\binom{N}{2} = N \cdot (N-1)/2$ ) and so forth. For a network with an odd number of species, this number is:

$$\#_{odd} = \binom{N}{0} + \binom{N}{1} + \dots + \binom{N}{\frac{(N-1)}{2}} = \sum_{i=0}^{(N-1)/2} \binom{N}{i} \quad (19)$$

Using the identity  $\binom{N}{k} = \binom{N}{N-k}$  and rearranging equation 19, we obtain:

$$\begin{aligned} \#_{odd} &= \frac{1}{2} \left( \left[ \binom{N}{0} + \binom{N}{N} \right] + \left[ \binom{N}{1} + \binom{N}{N-1} \right] + \dots + \left[ \binom{N}{\frac{(N-1)}{2}} + \binom{N}{\frac{(N+1)}{2}} \right] \right) \\ &= \frac{1}{2} \sum_{i=0}^N \binom{N}{i} \end{aligned} \quad (20)$$

Similarly, for a network with an even number of species, the number of possible patterns is:

$$\#_{even} = \binom{N}{0} + \binom{N}{1} + \dots + \binom{N}{\frac{N}{2}-1} + \frac{1}{2} \binom{N}{\frac{N}{2}} = \sum_{i=0}^{N/2-1} \binom{N}{i} + \frac{1}{2} \binom{N}{\frac{N}{2}} \quad (21)$$

Rearranging this expression as in the previous case we obtain:

$$\begin{aligned} \#_{even} &= \frac{1}{2} \left( \left[ \binom{N}{0} + \binom{N}{N} \right] + \dots + \left[ \binom{N}{\frac{N}{2}-1} + \binom{N}{\frac{N}{2}+1} \right] \right) + \frac{1}{2} \binom{N}{\frac{N}{2}} \\ &= \frac{1}{2} \sum_{i=0}^N \binom{N}{i} \end{aligned} \quad (22)$$

The identity  $\sum_{i=0}^N \binom{N}{i} = 2^N$  follows from the binomial formula. Introducing it in eqs.20-22 we arrive at the final result:

$$\#_{odd} = \#_{even} = \frac{1}{2} \sum_{i=0}^N \binom{N}{i} = 2^{N-1} \quad (23)$$

Next we demonstrate how to construct the networks that generate the patterns with each of the distribution of species in two phases. Further, this allows us to show how to construct all the networks that generate each of the  $2^{N-1}$  Turing patterns that can be formed by  $N$  species.

**Theorem** *The Turing network obtained by inverting the signs of all the incoming and outgoing edges of a particular node generates a pattern in which*



that node switches phase and the rest have the same phase than in the original. This transformation also preserves 1) the speed of pattern appearance 2) the wavelength of the pattern and the amplitude of the maximum and minimums of all the species.

*Proof.* The distribution of the species of a Turing network in two phases is determined by the eigenvector associated to the eigenvalue branch of  $\mathbf{F}^{\text{RD}}(q) = \mathbf{J}^R(r_0) - q^2 \mathbf{D}$  that has the maximum value for some  $q > 0$ . Let  $\lambda_q$  and  $\mathbf{v}(\lambda_q) = [v_1, \dots, v_i, \dots, v_N]^T$  be an eigenvalue and associated eigenvector of  $\mathbf{F}^{\text{RD}}(q)$ :

$$\mathbf{F}^{\text{RD}}(q) \cdot \mathbf{v} = \lambda_q \mathbf{v} \quad (24)$$

Precisely, two species are in phase if their components in the eigenvector have the same sign. Thus, the proof of this proposition requires showing the relationship between the eigenvector associated to  $\lambda_q$  in the original and transformed networks.

We define the reflection matrix  $L_I$  as the diagonal matrix that has  $-1$  in the  $i$ -th diagonal entry and  $+1$  in the rest. Note that from the definition of the reflection matrix,  $L_I$  is its own inverse:

$$L_I^{-1} \cdot L_I = L_I \cdot L_I^{-1} = \mathbf{I} \quad (25)$$

Applied to a vector  $\mathbf{v}$ , the reflection matrix  $L_I$  inverts the sign of the  $i$ -th component to  $\mathbf{v}' = L_I \cdot \mathbf{v} = [v_1, \dots, -v_i, \dots, v_N]^T$ . Applied to a square matrix  $\mathbf{A}$  the transformation  $\mathbf{A} \cdot L_I$  inverts the sign of the entries in the  $i$ -th column. Similarly, the transformation  $L_I^{-1} \cdot \mathbf{A}$  inverts the signs of the entries in the  $i$ -th row. The similarity transformation  $L_I^{-1} \cdot \mathbf{A} \cdot L_I$  inverts the signs of the

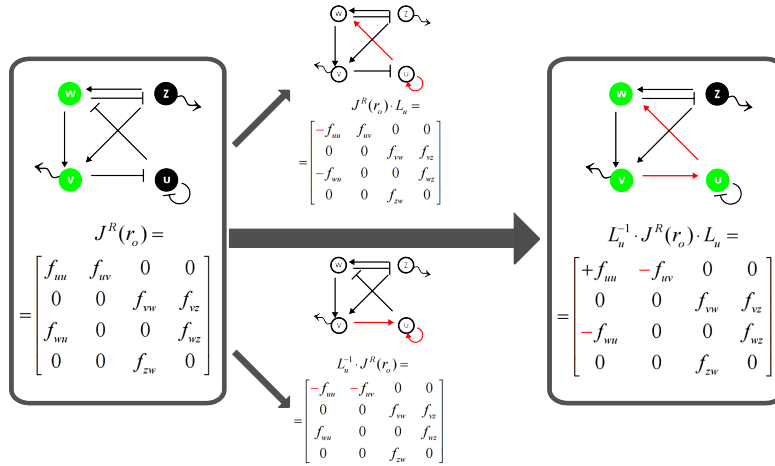


Figure 15: Illustration of the effect of reflection transformations applied to node  $u$  of an example network. Note that only the inversion of both incoming and outgoing edges results in a transformation that preserves the cycles signs. Nodes in phase plotted in the same color.

entries along the  $i$ -th column and  $i$ -th row, leaving the sign of the entry in the diagonal invariant. From the definition of the Coates graph of a reaction-diffusion equation, it follows that the transformation  $\mathbf{F}^{\text{RD}'} = L_I^{-1} \cdot \mathbf{F}^{\text{RD}} \cdot L_I$  is equivalent to changing the sign of all the edges that start or end in the  $i$ -th node, leaving the loop of node  $i$ , if it exists, invariant. The relationship between the eigenvectors of  $\mathbf{F}^{\text{RD}}$  and  $\mathbf{F}^{\text{RD}'}$  can now be obtained from eq.24:

$$\begin{aligned} \mathbf{F}^{\text{RD}}(q) \cdot (L_I \cdot L_I^{-1}) \cdot \mathbf{v} &= \lambda_q \cdot (L_I \cdot L_I^{-1}) \cdot \mathbf{v} \\ L_I^{-1} \cdot \mathbf{F}^{\text{RD}}(q) \cdot (L_I \cdot L_I^{-1}) \cdot \mathbf{v} &= \lambda_q \cdot L_I^{-1} \cdot (L_I \cdot L_I^{-1}) \cdot \mathbf{v} \\ (L_I^{-1} \cdot \mathbf{F}^{\text{RD}}(q) \cdot L_I) \cdot (L_I^{-1} \cdot \mathbf{v}) &= \lambda_q \cdot (L_I^{-1} \cdot \mathbf{v}) \\ \mathbf{F}^{\text{RD}'}(q) \cdot \mathbf{v}' &= \lambda_q \mathbf{v}' \end{aligned} \quad (26)$$

Therefore, the eigenvector of the transformed system in which the sign of all the edges that start or end in node  $i$  are inverted is:

$$\mathbf{v}' = L_I^{-1} \cdot \mathbf{v} = L_I \cdot \mathbf{v} = [v_1, \dots, -v_i, \dots, v_N]^T \quad (27)$$

This demonstrates that the  $i$ -th species switches phase and completes the proof. The inversion of the signs of the incoming and outgoing edges of a node is a similarity transformation, which leaves the characteristic polynomial, eigenvalues and dispersion relationship invariant. This means that the dynamical properties of the original and transformed network are identical because the wavelength, speed of pattern emergence and amplitudes of the pattern are invariant. Further, this type of transformation can be applied repeatedly to any combination of nodes to obtain all possible pairwise combinations of species in the two phases. This shows how, from a fixed  $N$ -node topology and invariant sign distribution of its cycles, it is possible to construct all the networks that generate the  $2^{N-1}$  possible Turing patterns.

As a final remark, it is worth emphasizing that this result is general: it does not depend on the size of the network and it does not require the network to be minimal. The key element is that this transformation changes the sign of the edges at node  $i$ , but it leaves the sign of all the cycles that pass through it invariant. This result showcases the power of analyzing Turing networks in this graph-theoretical framework, since it provides an almost trivial proof of a result that has not been shown before.

## 8 Rule of thumb to predict pattern phases

The topology of a minimal Turing network allows to predict the phases of the pattern produced. The simple method that we have found is based on examining the cycles of the network. Hence, it does not require to calculate the eigenvectors of the associated eigenvalue problem. This is particularly advantageous in networks with more than two species, where the analytical solution of the eigenvalue problem is either very cumbersome or, for  $N \geq 5$  cannot be found in terms of radicals. Numerical solutions can of course always be found, but they do not provide an intuitive understanding. In addition, in many real systems the values of the parameters are not known.

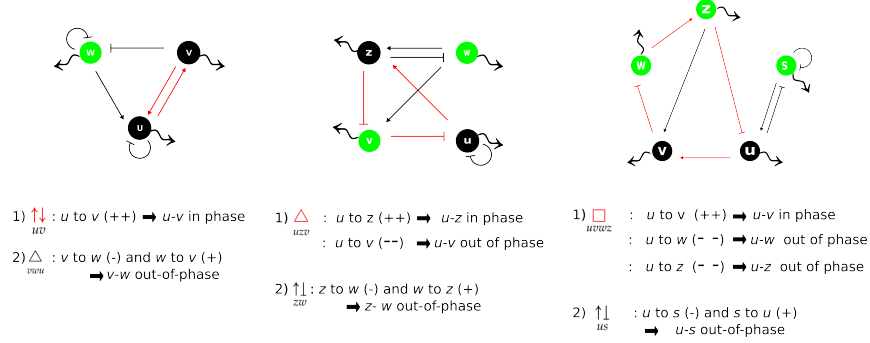


Figure 16: Examples of the application of the method to establish the phases of the Turing pattern without calculation of the eigenvectors. Positive cycle in destabilizing module in red. Nodes in-phase are filled in the same color.

The phase of the species in the positive cycle of the destabilizing factor is established first. For any two nodes  $a$  and  $b$ , the positive cycle connecting them can be divided into two directed paths, one from  $a$  to  $b$  and another from  $b$  to  $a$ . Also necessarily, since the cycle is positive, these paths must either be both positive or both negative. In the former case  $a$  and  $b$  will be in phase, in the later, out-of-phase. By this simple procedure, the relative phase of every pair of species in the destabilizing module is established.

Next, the phases of the species outside the destabilizing module relative to those inside will be established. Select a node outside the destabilizing module and find a cycle that connects it with a node inside. If the cycle is positive, the phase can be established as before. If the cycle is negative, again there are just two possibilities for any two nodes  $a$  and  $b$  in it: either the path from  $a$  to  $b$  is negative and the path from  $b$  to  $a$  is positive or the opposite. Let  $a$  be the species in the destabilizing module and  $a$  the specie outside. If the path from  $a$  in to  $b$  is positive, then  $b$  is in phase with  $a$ . If the path from  $a$  to  $b$  is negative, then  $b$  is out-of-phase with  $a$ . By iteration of this procedure, it is then possible to establish the phase of all the remaining nodes in the network. This method allows to predict correctly the phases of minimal networks of up to 5 nodes, as shown in SM fig.16. In non-minimal networks, there may be more than one cycle of the same order connecting the nodes outside the destabilizing module with the nodes that induce it. In this case, there may be an ambiguity if the different connecting cycles have different signs. Then, the cycle chosen to establish the phase of nodes outside the destabilizing module should have the largest weight amongst them. We have validated this method with only a few examples of non-minimal networks. However, it remains to be proved rigorously in the general case of non-minimal networks.

## 9 Algebraic proof of the impossibility of Turing patterns in systems with all species diffusing at the same rate

A reaction-diffusion network in which *all* species diffuse requires differential diffusivity. This is a well known property of Turing networks; here we provide a simple proof that carries over for networks of any size. This proof is also meant to highlight that the algebraic method does not provide an insight into how the diffusion constraints of Turing systems can be relaxed.

The emergence of Turing patterns is determined by the sign of the eigenvalues of the following equation

$$P_q(\lambda') = \det[\lambda' \cdot \mathbf{I} - (\mathbf{J}^R(r_0) - q^2 \cdot \mathbf{D})] = 0 \quad (28)$$

where  $\mathbf{J}^R(r_0)$  is the jacobian of the reaction term in the reaction-diffusion equations. Let all the species in the network diffuse at the same rate  $d$ ; the diffusion term is the diagonal matrix  $\mathbf{D} = d \cdot \mathbf{I}$ . Then, the eigenvalue problem can be rewritten as:

$$P_q(\lambda') = \det[\lambda' \cdot \mathbf{I} - (\mathbf{J}^R(r_0) - q^2 d \cdot \mathbf{I})] = \det[(\lambda' + q^2 d) \cdot \mathbf{I} - \mathbf{J}^R(r_0)] = 0 \quad (29)$$

In turn, the eigenvalues of  $\mathbf{J}^R(r_0)$  are given by:

$$P_0(\lambda) = \det[\lambda \cdot \mathbf{I} - (\mathbf{J}^R(r_0))] = 0 \quad (30)$$

A Turing network is by definition stable without diffusion. This means that the eigenvalues of  $\mathbf{J}^R(r_0)$  have all negative real part. Comparing eqs.29-30, it follows that  $\lambda' = \lambda - q^2 d < \lambda < 0$  for  $q > 0$ , which completes the proof.

## 10 On Turing minimal networks

### 10.1 Conjecture about number of edges of minimal network

A minimal Turing network is a strongly connected network that has the minimum number of edges required to build a network that can be stable without diffusion and that can undergo diffusion-driven instabilities. The strongly connected property is imposed to discard networks with modules that are a readout of the rest of the network<sup>4</sup>. In a network with  $N$  nodes, stability without diffusion requires that there is at least one stabilizing  $\ell_R$ -subgraph of every size up to  $N$ . Additionally, a network that generates stationary Turing patterns must have a stabilizing  $\ell_R$ -subgraph of size  $K < N$  that forms the destabilizing module. Examples of minimal networks obtained with software RDNets [23] are shown in the following figure:

---

<sup>4</sup>A network is strongly connected if for each pair of nodes  $u$  and  $v$  there is a path from  $u$  to  $v$  and vice-versa. Equivalently, a network is strongly connected if it cannot be partitioned into two subsets  $S$  and  $T$  such that all the edges between them have the initial node in  $S$  and the terminal node in  $T$  [5]. This shows why disregarding networks that are not strongly connected allows to filter out networks with modules that are just a downstream readout of a core network

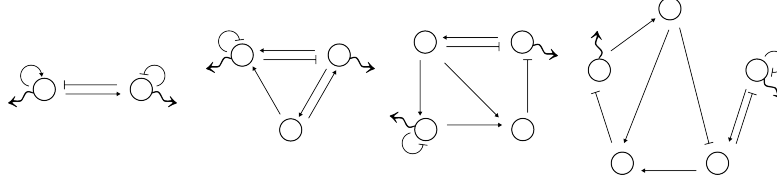


Figure 17: Examples of minimal Turing networks of  $N = 2, \dots, 5$  nodes

Interestingly, we find that in minimal Turing networks, the number of nodes  $N$ , the number of edges  $E$  and the number of cycles  $C$  are given by the following expression:

$$E = N + C - 1 \quad (31)$$

Thus, beyond the well known case of 2-node networks (which have 4 edges and 3 cycles), we find, surprisingly, that to build a minimal Turing network of  $N = 3, 4, 5$  nodes the number of cycles required is 4 in all cases (and the minimal number of edges is 6, 7 and 8). It is outside the scope of this work to assess whether the recurrence formula holds for  $N > 5$ . We leave it then as a conjecture<sup>5</sup>, noting the intriguing parallel with Euler's formula for the number of faces as a function of edges and faces in platonic solids and its connection with planar graphs [24].

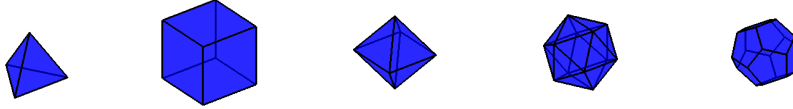


Figure 18: The number of faces  $F$ , vertex  $V$ , and edges  $E$  in the 5 platonic solids are given by Euler's formula:  $E = F + V - 2$ . Plot produced using Matlab script by Kevin Moerman.

However, aside from the interest as a theoretical problem, the fact that minimal Turing networks of  $N = 3, 4, 5$  have the same number of cycles should have interesting implications for their robustness. Cycles are the true variables that determine stability and diffusion-driven instabilities rather than individual kinetic parameters. However, the number of Hurwitz conditions associated to them grows with  $N$ . It then follows that larger minimal networks have the same number of degrees of freedom to fulfill a larger number of constraints (or in other words, that the parameters of larger Turing networks should be much more constrained). Interestingly, the fact that the stability space is a 4 dimensional space for  $N = 3, 4, 5$  could be used to compare the relative robustness of networks of different size.

<sup>5</sup>Our attempts to build a minimal network of 6 nodes with four cycles have been unsuccessful. It is likely that this is not possible, but the relationship between  $E, N, C$  might still hold if 5 cycles and 10 edges form the minimal Turing networks of 6 nodes.

## 10.2 Turing topological families of 4 nodes

There are 12 different minimal topological families of 4 nodes.

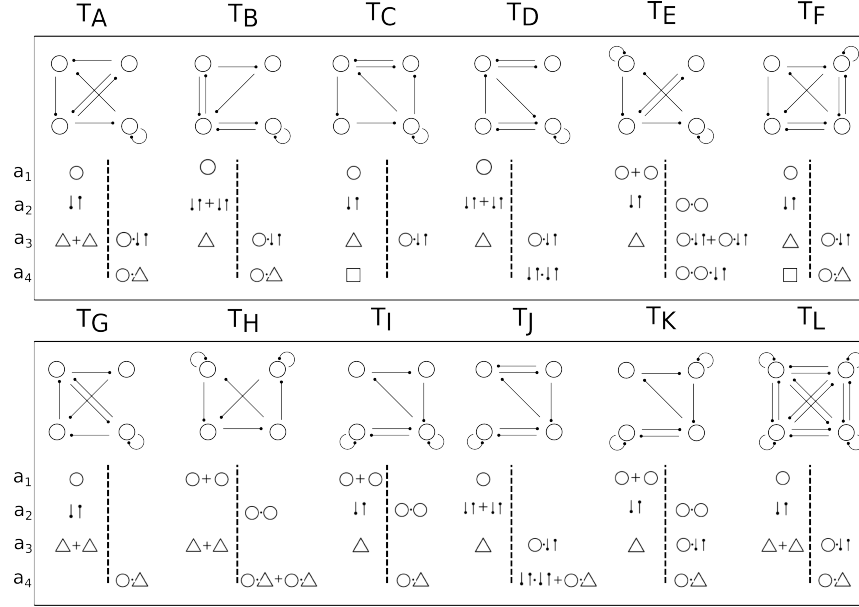


Figure 19: Turing networks of 4 Nodes can be classified in just 12 topological families.

As in the 3-node case, there are important variations between the Stability space of the different families. Also like in the 3-node case, setting one or more nodes as non-diffusible allows to relax the diffusion constraints. It is worth mentioning that this modification does not have the same effect in all families. For example, as shown before, only the  $T_B$  and  $T_J$  families have the specific structural properties that allow to obtain a Type-III networks with just one immobile node. Generally, while all topological families produce Type-I networks if all nodes are diffusible, the number of networks of other Types, Turing Filters and Turing oscillators obtained if nodes are immobile depends on the topological family. Importantly, strong relaxation of diffusion constrains and large robustness seems to be characteristic of specific families, whereas other families have small stability spaces or cannot produce Type-III networks. These features should be taken into account when choosing a design for an experimental Turing system.

## References

- [1] F.R. Gantmacher. *Applications Of The Theory Of Matrices*. Interscience Publishers, 1959.
- [2] Bruce L Clarke and Weimin Jiang. Method for deriving hopf and saddle-node bifurcation hypersurfaces and application to a model of the belousov-

- zhabotinskii system. *The Journal of chemical physics*, 99(6):4464–4478, 1993.
- [3] Maya Mincheva and Gheorghe Craciun. Multigraph conditions for multistability, oscillations and pattern formation in biochemical reaction networks. *Proceedings of the IEEE*, 96(8):1281–1291, 2008.
  - [4] C Coates. Flow-graph solutions of linear algebraic equations. *IRE Transactions on Circuit Theory*, 6(2):170–187, 1959.
  - [5] R.A. Brualdi and D. Cvetkovic. *A Combinatorial Approach to Matrix Theory and Its Applications*. Chapman and Hall/CRC, 2008.
  - [6] Xavier Diego. On the theory of cell migration: durotaxis and chemotaxis. *Universitat Politcnica de Catalunya, Ph.D Thesis*, 2013.
  - [7] R.A. Horn and C. R. Johnson. *Matrix Analysis*. Cambridge University Press, February 1990.
  - [8] Razvan A. Satnoianu, Michael Menzinger, and Philip K. Maini. Turing instabilities in general systems. *Journal of Mathematical Biology*, 41:493–512, 2000. 10.1007/s002850000056.
  - [9] L. Wang and M. Y. Li. Diffusion-driven instability in reaction-diffusion systems. *Journal of Mathematical Analysis and Applications*, 254(1):138 – 153, 2001.
  - [10] G. W. Cross. Three types of matrix stability. *Linear Algebra and its Applications*, 20(3):253 – 263, 1978.
  - [11] HG Othmer. Synchronized and differentiated modes of cellular dynamics. In *Dynamics of synergetic systems*, pages 191–204. Springer, 1980.
  - [12] R. B. Kellogg. On complex eigenvalues of m and p matrices. *Numerische Mathematik*, 19:170–175, 1972. 10.1007/BF01402527.
  - [13] R. A. Satnoianu and P. van den Driessche. Some remarks on matrix stability with application to turing instability. *Linear Algebra and its Applications*, 398:69 – 74, 2005. Special Issue on Matrices and Mathematical Biology.
  - [14] Istvan Lengyel and Irving R Epstein. A chemical approach to designing turing patterns in reaction-diffusion systems. *Proceedings of the National Academy of Sciences*, 89(9):3977–3979, 1992.
  - [15] Judit Horvth, Istvn Szalai, and Patrick De Kepper. An experimental design method leading to chemical turing patterns. *Science*, 324(5928):772–775, 2009.
  - [16] Vincent Castets, Etienne Dulos, Jacques Boissonade, and Patrick De Kepper. Experimental evidence of a sustained standing turing-type nonequilibrium chemical pattern. *Physical Review Letters*, 64(24):2953–2956, 1990.
  - [17] Istvan Lengyel and Irving R Epstein. Modeling of turing structures in the chloriteiodidemalonic acidstarch reaction system. *Science*, 251(4994):650–652, 1991.

- [18] Erik M Rauch and Mark M Millonas. The role of trans-membrane signal transduction in turing-type cellular pattern formation. *Journal of theoretical biology*, 226(4):401–407, 2004.
- [19] Herbert Levine and Wouter-Jan Rappel. Membrane-bound turing patterns. *Physical Review E*, 72(6):061912, 2005.
- [20] K Korvasov, EA Gaffney, PK Maini, MA Ferreira, and V Klika. Investigating the turing conditions for diffusion-driven instability in the presence of a binding immobile substrate. *Journal of theoretical biology*, 367:286–295, 2015.
- [21] Vclav Klika, Ruth E Baker, Denis Headon, and Eamonn A Gaffney. The influence of receptor-mediated interactions on reaction-diffusion mechanisms of cellular self-organisation. *Bulletin of mathematical biology*, 74(4):935–957, 2012.
- [22] Chunyan Mou, Ben Jackson, Pascal Schneider, Paul A Overbeek, and Denis J Headon. Generation of the primary hair follicle pattern. *Proceedings of the National Academy of Sciences*, 103(24):9075–9080, 2006.
- [23] Luciano Marcon, Xavier Diego, James Sharpe, and Patrick Mller. High-throughput mathematical analysis identifies turing networks for patterning with equally diffusing signals. *eLife*, 5:e14022, 2016.
- [24] Harold Scott Macdonald Coxeter. *Regular polytopes*. Courier Corporation, 1973.